SISSA ISAS

INTERNATIONAL SCHOOL FOR ADVANCED STUDIES

Condensed Matter Sector

Efficient calculation of RPA correlation energy in the Adiabatic Connection Fluctuation-Dissipation Theory

Thesis submitted for the degree of
Doctor Philosophiæ

Candidate
Huy-Viet Nguyen

Supervisor
Prof. **Stefano de Gironcoli**

October 2008

Contents

List of Figures

List of Tables

Introduction

Since its theoretical foundation established in the 1960s [1, 2], Density Functional Theory (DFT) has increasingly gained attention, and, in fact, has become nowadays a standard tool for electronic structure calculations of atoms, molecules, solids and complex materials. Although DFT is an exact theory for ground state properties for any electronic system, an approximate treatment of the so-called exchange-correlation (xc) energy is required in practical applications. DFT with two widely-used approximations, namely the Local (Spin) Density Approximation (LSDA) [2, 3] and (many flavors of) Generalized Gradient Approximations (GGA) [4], has given many spectacular successes in predicting and explaining the properties of electronic systems, such as cohesion, bonding, structures, vibrations, etc. There exist many systems, however, where DFT within LDA and GGAs performs poorly, if not fails completely. They can be divided into two classes: sparsely packed systems having small overlapping density where long range correlation effects are important, and strongly correlated systems. The failure of DFT in the latter is attributed to the strong and localized electron-electron interaction that makes the non-interacting electron picture become not suitable. As for the former, the poor performance is due to the local (LDA) or semi-local (GGAs) nature of these approximations which obviously can not give a good description of systems with important long-range correlation effects. These kinds of systems are frequently met in nature, e.g. in bio-molecules, as well as in physical and chemical processes, such as, for instance, in absorption on surfaces, chemical reactions, etc.

During the past decade, many attempts have been done to improve performance of DFT in description of sparsely packed systems. The natural way is to include non-local

correlations, an important ingredient missing in both LDA and GGAs. Obviously the picture of a slowly varying density, that is the basis in the development of LDA and GGAs, does not help much. In searching for a truly non-local functional, the Adiabatic-Connection Fluctuation-Dissipation (ACFD) [7] theory plays a special role. In this formalism, the exchange-correlation (xc) energy can be expressed in an exact formula through dynamic response functions of all fictitious systems which connect the non-interacting Kohn-Sham (KS) system with the real many-body interacting one. The formalism provides not only a theoretical framework for systematic developments of truly non-local functional but also a practical way to calculate xc-energy accurately. In fact, all of the limited number of successful DFT descriptions of van der Waals systems start with the exact expression of correlation energy derived from this formalism. These descriptions ranges from crude approximations using electron-gas local response functions [8, 9] to the direct evaluation of the exact formula for the correlation energy which is unfortunately very demanding [10, 11, 12, 13, 15].

In the former approach, the exact adiabatic-connection formula for the correlation energy is simplified in term of the dielectric function which is then approximated by using locally the dielectric function of the homogeneous electron gas calculated for the local density [8]. This approach has been applied to study a number of van der Waals bound systems with some successes. In a few first applications, the correlation energy was obtained from post-DFT perturbative calculations, i.e. without any self-consistency. Very recently [9], the procedure has been made self-consistent although it is still much more expensive than standard DFT. In our opinion, this approach could demonstrate to be a practical way to overcome the limitation of LDA-GGA-type functionals in many systems. However, more calculations need to be performed to validate the method. As for the latter, correlation energy is also calculated in a post-DFT procedure but without any simplification of the adiabatic connection formula. Exchange and correlation are thus treated on the same footing in this approach. Despite of the fact that one still needs an approximation for xc-kernel, it has been shown that by using the Random Phase Approximation (RPA) – the most computationally convenient approximation – plus a

local-density correction for short range correlation, one ends up with a reasonably good description of the van der Waals energy [12, 13, 15]. This type of calculation is, however, computationally very demanding which is the most important practical limitation of this approach.

In our opinion, more calculations and further developments need to be pursued in order to explore the potential offered by an approximate treatment of ACFD formula for the calculation of accurate exchange-correlation energies. In the present thesis, we will present our approach, from both computational and physical point of views, aiming at building a realistic, computationally efficient description of van der Waals, or, in general, long range correlations, in DFT based on ACFD formula. We will present our implementation for direct evaluation of RPA correlation energy based on calculation of eigenvalues of response functions which has several advantages comparing to existing implementation. We will also investigate the possibility to simplify the description of frequency-dependent response function, the key quantity in the calculation of the correlation energy in ACFD formalism, by using Thomas–Fermi–von Weizsäcker (TFvW) approximation for kinetic energy functional.

The thesis is organized as follows. After this short Introduction, we will present in Chapter 1 basic concepts of electronic structure theory with emphasis on Density Functional Theory in the plane-wave pseudopotential approach. The failure of LDA and GGAs for van der Waals systems and the need for the development of new approaches will be discussed at the beginning of Chapter 2. We then will recall the formalism by which exchange and correlation energies of an electronic system can be expressed in term of linear response functions through an exact formula. Our efficient implementation for the calculation of correlation energy in the RPA is also described here with some technical details of its implementation in plane-wave pseudopotential method. To validate the implementation and to improve its efficiency, we have chosen bulk silicon system as the test ground to perform a detailed analysis of relevant issues. We will then apply our approach to study the system of Beryllium dimer where LDA or GGA fails qualitatively. Although EXX/RPA+ study of this system has been performed in the past [12], we will

show that our calculation is more accurate and the result will demonstrate that in fact special care must be taken in the calculation of both exact-exchange and RPA correlation energies. Chapter 3 will be devoted to the discussion of approximate linear response functions using the non-interacting Thomas–Fermi–von Weizsäcker kinetic energy functional. Applications of the methods described in Chapter 2 and Chapter 3 to study some test cases will be shown in Chapter 4. We will first present the results and comparisons for the asymptotic long-range interactions via van der Waals coefficients of atoms and molecules calculated both from exact and approximate response functions. We will also demonstrate the efficiency of our implementation of ACFD formula for the calculations of correlation energy of atomic systems. The potential of TFvW approximation to capture the essence of long range correlations will be discussed on the basis of the results of correlation energies obtained for atomic and molecular systems.

Chapter 1

Basics of electronic structure calculations

1.1 Theory of electronic structure

Quantum mechanical simulations of electrons and ions is no doubt one of the most powerful tools that people have at present for explaining and predicting a vast range of phenomena in (low-energy) physics, chemistry and biology. In quantum theory, electrons and ions are described by a mathematical object called wave function. Although the wave function does not represent any physical quantity, its square modulus is interpreted as the probability density of the distribution of particles. The distribution, or more generally the dynamics, of electrons and ions is the key ingredient for understanding the behaviors of the systems they constitute.

1.1.1 Schrödinger equation

From the theoretical point of view, knowing the wave function is enough to describe all the properties of the systems. It is postulated that the wave function is the solution of the well-known Schrödinger wave equation

$$\hat{H}\Psi = W\Psi, \tag{1.1}$$

where Ψ and W are the wave function and total energy of the system, respectively. The non-relativistic Hamiltonian $\hat{H}$ is written explicitly for systems consisting of N electrons and M nuclei as

$$\begin{aligned}\hat{H} &= \hat{T}_e + \hat{U}_{e-e} + \hat{W}_{e-n} + \hat{T}_n + \hat{W}_{n-n} \\ &= \sum_{i=1}^{N}\left(-\frac{\hbar^2}{2m_e}\nabla_i^2 + v(\mathbf{r}_i)\right) + \frac{e^2}{2}\sum_{i\neq j}\frac{1}{|\mathbf{r}_i - \mathbf{r}_j|} + \hat{T}_n + \hat{W}_{n-n},\end{aligned} \tag{1.2}$$

with

$$v(\mathbf{r}_i) = -\sum_{\alpha}\frac{e^2 Z_\alpha}{|\mathbf{r}_i - \mathbf{R}_\alpha|} \quad \text{and} \quad \hat{W}_{n-n} = \frac{e^2}{2}\sum_{\alpha\neq\beta}\frac{Z_\alpha Z_\beta}{|\mathbf{R}_\alpha - \mathbf{R}_\beta|}. \tag{1.3}$$

The operators in (1.2) are associated, respectively, with the kinetic energy $\hat{T}_e$ of electrons, electron-electron interaction energy $\hat{U}_{e-e}$, the potential energy $\hat{W}_{e-n}$ of electrons moving in the field of nuclei of charge Z_α, the kinetic energy $\hat{T}_n$ of nuclei, and the Coulomb interaction energy $\hat{W}_{n-n}$ between nuclei. Equation (1.1) is an eigenvalue equation for N-electron-M-nucleus many-body wave function $\Psi(\mathbf{r}_1, ..., \mathbf{r}_N; \mathbf{R}_1, ..., \mathbf{R}_M)$ with Hermitian operator $\hat{H}$. The Hamiltonian is too complicated for a direct handling, neither analytically nor numerically. Approximations are therefore needed for more realistic and practical descriptions.

1.1.2 The Born-Oppenheimer approximation

In finding a possible simplification of the full N-electron-M-nucleus Hamiltonian, a natural question comes out first: Since electrons and nuclei are very different, is it possible to handle them separately? The answer, to a very good approximation, is yes. This is the well-known *adiabatic* or Born-Oppenheimer approximation [16]. The physical reason for the excellent accuracy of this approximation rests on the fact that electron mass is much smaller than that of nuclei (usually $\frac{m_e}{M}$ is between 10^{-4} and 10^{-5}). As a consequence, the typical electronic time scale is much shorter than that of nuclei and the dynamics of the system can be obtained, to a good approximation, by first considering the nuclei fixed at positions $\mathbf{R}_1, \mathbf{R}_2, ..., \mathbf{R}_M$ and determining the corresponding ground state (GS) energy of electrons, $E_{el}(\{\mathbf{R}_i\}$. Then the electrons no longer appear explicitly in the equation of

motion for the nuclei which is determined by the nuclear kinetic energy and an effective potential $E_{el}(\{\mathbf{R}_i\}) + E_{nuc}(\{\mathbf{R}_i\})$, which is called *(GS) Born-Oppenheimer potential energy surface*. Mathematically, this approximation allows to write the total wave function as the product of the wave function of nuclei and electrons

$$\Psi(\{\mathbf{r}_i\}, \{\mathbf{R}_i\}) = \Phi(\{\mathbf{R}_i\})\psi(\{\mathbf{r}_i\}; \{\mathbf{R}_i\}), \tag{1.4}$$

where $\Phi(\{\mathbf{R}_i\})$, in the *adiabatic* approximation, is the solutions of the equation

$$\left(-\frac{\hbar^2}{2M_\alpha}\sum_{\alpha=1}^{M}\nabla_\alpha^2 + E_{el}(\{\mathbf{R}_i\}) + E_{nuc}(\{\mathbf{R}_i\})\right)\Phi(\{\mathbf{R}_i\}) = \mathcal{E}\Phi(\{\mathbf{R}_i\}), \tag{1.5}$$

and $\psi(\{\mathbf{r}_i\}; \{\mathbf{R}_i\})$ satisfies the Schrödinger equation for the electrons in the fixed positions of the nuclei

$$\left(-\frac{\hbar^2}{2m_e}\sum_{i=1}^{N}\nabla_i^2 - \sum_{i=1}^{N}\sum_{\alpha=1}^{M}\frac{e^2 Z_\alpha}{|\mathbf{r}_i - \mathbf{R}_\alpha|} + \sum_{i=1}^{N}\sum_{j>i}^{N}\frac{e^2}{|\mathbf{r}_i - \mathbf{r}_j|}\right)\psi(\{\mathbf{r}_i\}; \{\mathbf{R}_i\}) = E_{el}(\{\mathbf{R}_i\})\psi\left(\{\mathbf{r}_i\}; \{\mathbf{R}_i\}\right), \tag{1.6}$$

and depends parametrically on the atomic positions $\{\mathbf{R}_i\}$ only through the external potential. Although, the Born-Oppenheimer theorem allows to work with the much simpler problem of considering motions of electrons and nuclei separately, the problem of the electrons only itself is still a many-body problem. Solving the equation for electrons (1.6) is the main task of computational electronic structure theory.

1.1.3 Methods for quantitative electronic calculations

Due to the presence of non-local Coulomb interaction, there is no way to solve this many-body Hamiltonian directly by analytical methods, even for the simplest case of Helium atom. On the contrary, numerical methods for finding the ground state solution working directly with this Hamiltonian is possible. The very first quantitative calculations for atomic systems had been done soon after the advent of quantum mechanics, as, for instance, variational calculation of ground state of Helium atom by E. A. Hylleraas [18], or self-consistent field calculation by D. R. Hartree [17] (later improved to include exchange effect by V. Fock [19] forming the well-known Hartree-Fock method which is still

widely-used nowadays. These early calculations are prototypes of many modern methods for electronic structure calculation. The greatest challenge of electronic structure theory is the electron correlation. Although the effect of correlation through the Pauli exclusion principle, the electron exchange, is properly treated in Hartree-Fock method, total electronic energy includes additional correlation originating from electron-electron interaction which, in many cases, is very important and difficult to describe. Correlated methods often used by the quantum chemistry community, such as Configuration Interaction (CI), Many-Body Perturbation Theory (MBPT), while giving accurate description of electron correlation, are very expensive and can be applied to study systems with a number of electrons not larger than a few tens even with modern computational facilities. Mean-field independent-particle methods are rather cheap compared to the correlated ones. However, their early developments usually did not give very accurate results since correlation due to electron-electron interaction was not taken into account. The advent of Density Functional Theory in the 1960s, with a constantly improved quality of exchange-correlation functionals and with many technical developments for solving the independent-particle equations, has made it the most widely used approach for quantitative calculations on realistic problems in physics, chemistry and materials science nowadays.

1.2 Density Functional Theory

Unlike other mean-field independent-particle methods, the one based on density functional theory gives, in principle, an exact description of the electronic ground state. Approximation is then needed in practical applications, but in the elegant formulation of Kohn and Sham [2] both exchange and correlation effects are taken into account which make it supersede other approaches. Contrary to traditional many body wave-function methods where a mathematical quantity, the wave function, is used to describe the electronic system, in DFT, a measurable physical quantity, the electronic density, is used as the solely needed variable. This has a conceptual advantage because when the number of electron in the system increases, the wave function, which depends on $3N$ variables for a system of N

electrons, becomes a very complicated object while the electronic density always depends only on 3 spatial variables. The description of electronic system in term of density is made possible by the fact that *any property of a many-body interacting particles can be viewed as a functional of the ground state density* [1].

The idea of using the density to describe properties of electronic systems had actually appeared in the work by Thomas and Fermi long before the foundation of DFT [20, 21]. At that time, it was not known whether the energy functional could be formally written in terms of the density only, and, in fact, the energy functional was derived from the heuristic argument. Since exchange and correlation among electrons were neglected in the theory, it is not accurate enough for practical purposes. However, the extension by Dirac [22] to include a local approximation for exchange, which is still in use today, did not help much because the local-density approximation for the kinetic energy adopted in the Thomas-Fermi theory is too crude.

1.2.1 The Hohenberg-Kohn theorems

Hohenberg and Kohn have proven two theorems allowing to formulate density functional theory as an exact theory of many-body systems [1]. This remarkable result of DFT was proven by surprisingly simple *reductio ad absurdum* arguments. The first theorem states that the ground state density $n_0(\mathbf{r})$ of a bound system of interacting electrons in some external potential $V_{ext}(\mathbf{r})$ determines this potential uniquely up to an additive constant. This means that $n_0(\mathbf{r})$ determines both the number of electrons N and the external potential $V_{ext}(\mathbf{r})$, the quantities which fix the Hamiltonian. Therefore, $n_0(\mathbf{r})$ determines implicitly all properties which are derivable from the Hamiltonian of the system. The second Hohenberg and Kohn theorem states that the ground state energy, the most important property of the electronic ground state, is a functional of $n_0(\mathbf{r})$ and satisfies a variational principle, i.e. $n_0(\mathbf{r})$ minimizes the following energy functional

$$E[n(\mathbf{r})] = F[n(\mathbf{r})] + \int d\mathbf{r} V_{ext}(\mathbf{r}) n(\mathbf{r}), \tag{1.7}$$

where $F[n] = T[n] + E_{int}[n]$ includes all internal energies (kinetic and potential) and is a universal functional (in the sense that it is independent of the external potential $V_{ext}(\mathbf{r})$). Unfortunately the Hohenberg and Kohn theorem gives no information about how to construct this universal functional for an interacting system. All direct approximations of this functional in term of the density alone, e.g. the Thomas-Fermi-Dirac theory, give poor results. It is the approach proposed by Kohn and Sham in 1965 that has made DFT the most widely used method for electronic structure calculations.

1.2.2 The Kohn-Sham equations

In a seminal paper follow the theoretical foundation of DFT, Kohn and Sham [2] developed a good approximation for the functional $F[n]$ by introducing an auxiliary system of non-interacting electrons which has the same ground state density as the interacting one. In this way the functional $F[n]$ can be decomposed as

$$F[n] = T_s[n] + \frac{e^2}{2}\int \frac{n(\mathbf{r})n(\mathbf{r}')}{|\mathbf{r}-\mathbf{r}'|}d\mathbf{r}d\mathbf{r}' + E_{xc}[n], \tag{1.8}$$

where the first term $T_s[n]$ is the kinetic energy of the non-interacting system, the second one is the classical electrostatic interaction energy of the electronic density distribution (including the self-interaction), and the last one is called the *exchange-correlation energy*, E_{xc}, and is *defined* by equation (1.8) itself. More explicitly, E_{xc} can be written as

$$E_{xc}[n] = T[n] - T_s[n] + V_{ee}[n] - \frac{e^2}{2}\int \frac{n(\mathbf{r})n(\mathbf{r}')}{|\mathbf{r}-\mathbf{r}'|}d\mathbf{r}d\mathbf{r}'. \tag{1.9}$$

In this form, it is clearer that all many body effects are included in E_{xc}. Minimizing the energy functional $E[n]$ defined by equation (1.7), with the constraint that the integration of the density gives the correct number of electrons, is equivalent to solving the set of

self-consistent equations, called the Kohn-Sham equations

$$
\begin{aligned}
-\frac{\hbar^2}{2m}\nabla^2\psi_i(\mathbf{r}) + V_{KS}(\mathbf{r})\psi_i(\mathbf{r}) &= \epsilon_i\psi_i(\mathbf{r}), \\
V_{KS}(\mathbf{r}) &= V_{ext}(\mathbf{r}) + V_H(\mathbf{r}) + V_{xc}(\mathbf{r}), \\
V_H(\mathbf{r}) = \int \frac{n(\mathbf{r}')}{|\mathbf{r}-\mathbf{r}'|}d\mathbf{r}', &\qquad V_{xc}(\mathbf{r}) = \frac{\delta E_{xc}(n)}{\delta n(\mathbf{r})}, \\
n(\mathbf{r}) &= \sum_{i\in occ.} |\psi_i(\mathbf{r})|^2.
\end{aligned}
\tag{1.10}
$$

This is a nonlinear system of equations because the Kohn-Sham potential V_{KS} depends on the solutions $\{\psi_i\}$ through the dependence of the Hartree and exchange-correlation potential (V_H and V_{xc}) on density $n(\mathbf{r})$. Once the functional $E_{xc}[n(\mathbf{r})]$ is explicitly defined, the Kohn-Sham equation can be solved self-consistently, for instance, by a variety of numerical methods. It is worth mentioning that the self-consistent solution of the Kohn-Sham equations in two widely used LDA and GGA approximations for the xc-functional is minimally more difficult than the solution of the Hartree equation and much easier than the solution of the Hartree-Fock equations. This makes the method computationally attractive.

1.2.3 Approximation for exchange-correlation functional

So far DFT has been presented as a mathematically exact formulation of electronic structure from the perspective of the electronic density $n(\mathbf{r})$. On a concrete calculation, a practical approximation for functional $F[n(\mathbf{r})]$ in the Hohenberg-Kohn formulation, and for $E_{xc}[n(\mathbf{r})]$ in the Kohn-Sham formulation is needed. Clues for finding an efficient approximation are obviously out of DFT scope; they must come from the physics of electronic structure. It is intriguing to write the exchange-correlation functional as

$$
E_{xc}[n(\mathbf{r})] = \int \epsilon_{xc}(\mathbf{r}; [n(\tilde{\mathbf{r}})])n(\mathbf{r})d\mathbf{r}, \tag{1.11}
$$

where $\epsilon_{xc}(r; [n(\tilde{\mathbf{r}})])$, a *functional* of density $n(\tilde{\mathbf{r}})$, represents an exchange-correlation energy per particle at point $\mathbf{r}$. In the limit of the homogeneous electron gas, the effects of exchange and correlation are local in character; ε_{xc} is a *function* of the density which is a constant

over the whole space for this specific system[1]. Naturally the same function would be a good approximation for an inhomogeneous system with slowly varying density when applying locally this functional form (thus the name Local Density Approximation.) As pointed out in the original paper by Kohn and Sham, solids can often be viewed as close to the limit of homogeneous electron gas. And experience has shown that LDA and its extension to deal with spin-polarized systems (LSDA) work remarkably well. The success of LDA when applied to solids (and also atomic or molecular systems to a lesser extent) is far more than originally expected, regardless of inhomogeneity of these systems. For weakly correlated materials like semiconductors and simple metals, LDA gives accurate descriptions of structural and vibrational properties: lattice constants, bulk moduli and phonon vibrational frequencies are typically accurate to within a few percent. For cohesive energies of solids, dissociation energies of molecules and ionization energies of atoms, the LDA gives less accurate results, typically within $10 - 20\%$. In modern implementation of LDA, the functional form of the correlation energy density is parametrized from the very accurate data calculated by using Quantum Monte Carlo methods [23] and can be considered an exactly known function.

The success of LDA has led to the development of many extensions by including also the gradient of the density into the functional, resulting in various Generalized Gradient Approximations (GGAs) [4], which, in many cases, give remarkable improvement over the LDA, especially for cohesive and dissociation energies. Another approach for the extension of LDA is the hybrid method proposed by A. Becke in 1993 [5]. A hybrid functional incorporates a portion of exact exchange from Hartree-Fock theory with exchange and correlation from other sources, e.g. in LDA or GGAs. This approach is particularly useful when energetics is concerned and is used popularly in the chemistry community.

[1]The form of the function was already known, though not very accurately, before the seminal work of Kohn and Sham.

1.3 Solving Kohn-Sham equations: Plane-wave pseudopotential method

The Kohn-Sham equations (1.10) can be solved, for a periodic system, either by using a discretized form of the linear differential operators and orbitals on a grid in real space or by expanding the orbitals in a complete set of known functions called a basis set, such as, for example Gaussian functions, atomic orbitals, plane-waves, etc. By expanding into a basis set, the integro-differential KS equations are transformed into the algebraic ones, which can be solved by a variety of available numerical methods. Among various options for solving the Kohn-Sham equation using a basis set, we restrict our discussion to the case of plane waves (PW).

The Plane-Wave basis set. Plane-wave basis set has many advantages: the matrix elements of the Hamiltonian are simple, the basis functions are orthonormal by definition, unbiased by the atomic positions so that they give the same accuracy at every points in space and thus having the ability to accurately describe different kinds of structure. The convergence of the calculation with respect to the quality (in this case is the size) of the truncated basis set can be simply checked by increasing the kinetic energy cutoff used to define which plane waves are included in the basis. Besides these attractive features, the existence of fast Fourier transform (FFT) algorithms [24] gives computational advantages to plane-wave basis set. Because the potential term in equation (1.10) is diagonal in real space while the kinetic term of the same equation is so in reciprocal space, this algorithm allows a fast transformation from one to the other space and vice versa thus allowing an efficient application, for instance, of the Kohn-Sham Hamiltonian to a trial wave function.

The basis of orthonormal plane waves consists of functions

$$|\mathbf{q}\rangle = \frac{1}{\sqrt{\Omega}} \exp(i\mathbf{q}.\mathbf{r}), \tag{1.12}$$

where Ω is the volume. The orthonormality property requires the condition

$$\langle \mathbf{q}'|\mathbf{q}\rangle \equiv \frac{1}{\Omega}\int_{\Omega} \exp(-i\mathbf{q}'.\mathbf{r}) \exp(i\mathbf{q}.\mathbf{r}) d\mathbf{r} = \delta_{\mathbf{q},\mathbf{q}'}. \tag{1.13}$$

Kohn-Sham equation in the plane-wave basis set. In a periodic system, the orbitals can be required to be normalized and obey the periodic boundary conditions. Using the fact that any periodic functions can be represented by a set of Fourier components, the eigenfunctions of the Kohn-Sham equation (also called Kohn-Sham orbitals) can be written as

$$\psi_i(\mathbf{r}) = \sum_{\mathbf{q}} c_{i,\mathbf{q}}.\frac{1}{\sqrt{\Omega}}\exp(i\mathbf{q}.\mathbf{r}) \equiv \sum_{\mathbf{q}} c_{i,\mathbf{q}}|\mathbf{q}\rangle \tag{1.14}$$

The KS equation (1.10) in Fourier space reads

$$\sum_{\mathbf{q}}\langle\mathbf{q}'|\hat{H}_{KS}|\mathbf{q}\rangle c_{i,\mathbf{q}} = \epsilon_i \sum_{\mathbf{q}}\langle\mathbf{q}'|\mathbf{q}\rangle = \epsilon_i c_{i,\mathbf{q}}. \tag{1.15}$$

The matrix elements of the KS Hamiltonian consists of two parts with different representation in Fourier space. The matrix element of the kinetic energy operator is simply derived

$$\langle\mathbf{q}'|-\frac{\hbar^2}{2m_e}\nabla^2|\mathbf{q}\rangle = \frac{\hbar^2}{2m_e}|q|^2\delta_{\mathbf{q},\mathbf{q}'}. \tag{1.16}$$

The potential $V_{KS}(\mathbf{r})$ is periodic and can be written as the sum of its Fourier components

$$V_{KS}(\mathbf{r}) = \sum_m V_{KS}(\mathbf{G}_m)\exp(i\mathbf{G}_m.\mathbf{r}), \tag{1.17}$$

where $\mathbf{G}_m$ are reciprocal lattice vectors, and

$$V_{KS}(\mathbf{G}) = \frac{1}{\Omega_{cell}}\int_{\Omega_{cell}} V_{KS}(\mathbf{r})\exp(-i\mathbf{G}.\mathbf{r}), \tag{1.18}$$

with Ω_{cell} the volume of the primitive cell. Therefore the matrix elements of the potential operator

$$\langle\mathbf{q}'|V_{KS}(\mathbf{r})|\mathbf{q}\rangle = \sum_m V_{KS}(\mathbf{G}_m)\delta_{\mathbf{q}'-\mathbf{q},\mathbf{G}_m}, \tag{1.19}$$

are not zero only if $\mathbf{q}$ and $\mathbf{q}'$ differ by a reciprocal lattice vector $\mathbf{G}_m$. If we introduce the vector $\mathbf{k}$ inside the first Brillouin zone such that $\mathbf{q} = \mathbf{k} + \mathbf{G}_m$ and $\mathbf{q}' = \mathbf{k} + \mathbf{G}_{m'}$, then the KS equation for a given $\mathbf{k}$ couples only the coefficients $c_{i,\mathbf{k}}, c_{i,\mathbf{k}+\mathbf{G}_1}, c_{i,\mathbf{k}+\mathbf{G}_2}, ...$ corresponding to plane waves whose wave vectors differ from $\mathbf{k}$ by a reciprocal lattice vector. Therefore, the original equation is separated into many independent equations, each of

them corresponding to a vector in the first Brillouin zone. Changing the summation index from $\mathbf{q}, \mathbf{q}'$ to m, m', the KS equation with a given $\mathbf{k}$ vector in matrix form reads

$$\sum_{m'} H_{m,m'}(\mathbf{k}) c_{i,m'}(\mathbf{k}) = \epsilon_i(\mathbf{k}) c_{i,m}(\mathbf{k}), \tag{1.20}$$

with

$$H_{m,m'}(\mathbf{k}) = \frac{\hbar^2}{2m_e}|\mathbf{k} + \mathbf{G}_m|^2 \delta_{m,m'} + V_{KS}(\mathbf{G}_m - \mathbf{G}'_m). \tag{1.21}$$

The eigenfunction $\psi_i(\mathbf{r})$ corresponding to a solution of (1.20) can be written

$$\psi_{i,\mathbf{k}}(\mathbf{r}) = \sum_m c_{i,m}(\mathbf{k}).\frac{1}{\sqrt{\Omega}} \exp(i(\mathbf{k} + \mathbf{G}_m).\mathbf{r}) = \exp(i\mathbf{k}.\mathbf{r})\frac{1}{\sqrt{N_{cell}}} u_{i,\mathbf{k}}(\mathbf{r}), \tag{1.22}$$

where $\Omega = N_{cell}\Omega_{cell}$ with N_{cell} and Ω_{cell} being the number of primitive cells in the volume Ω and the volume of primitive cell respectively and

$$u_{i,\mathbf{k}}(\mathbf{r}) = \frac{1}{\sqrt{\Omega_{cell}}} \sum_m c_{i,m}(\mathbf{k}) \exp(i\mathbf{G}_m.\mathbf{r}) \tag{1.23}$$

It is obvious that $u_{i,\mathbf{k}}(\mathbf{r})$ has the periodicity of the crystal and equation (1.22) is nothing but the well-known Bloch theorem. We have seen that the KS equation (1.20) is independent for each $\mathbf{k}$ vector in the first Brillouin zone. The eigenstates therefore can be labelled by the wave vector $\mathbf{k}$. At each $\mathbf{k}$ there is a discrete set of eigenstates labelled by $i = 1, 2, 3, ...$ In the limit of macroscopic system (large Ω), the allowed values of $\mathbf{k}$ become very dense and the set of eigenvalues $\epsilon_i(\mathbf{k})$ become a continuous bands.

In principle, expansion coefficients and hence Kohn-Sham eigenstates at each k-point are obtained from the solutions of the eigenvalue problem (1.20) in the basis of discrete but infinite number of plane waves with wave vectors $\mathbf{k} + \mathbf{G}_m$. In practice, it is not really so because one can take advantage of the fact that at high energy the Hamiltonian is kinetic-energy dominated thus making high wave-vector components in the plane wave expansion of the smooth and slowly varying valence functions small. The number of plane waves needed to have a good representation of the occupied orbitals is therefore small enough to make the numerical solution of Eq. (1.20) practical. Plane waves used in calculation are usually chosen to have kinetic energy smaller than a given value called

cut-off energy E_{cut}

$$\frac{\hbar^2}{2m_e}|\mathbf{k}+\mathbf{G}_m|^2 \leq E_{cut}. \tag{1.24}$$

As stated previously, convergence with respect to the number of plane waves can be easily checked by increasing E_{cut}.

In atoms and molecules, the charge density and the wave functions in the bonding and tail regions are slowly varying, and a plane-wave basis set could be used without any problem. However, they still vary strongly in the core region, and the number of plane waves needed to describe them well becomes intractable in practice. In order to use a plane wave basis set, the core region needs to be treated in a different way. This is done in the pseudopotential approximation briefly mentioned in the next section.

Pseudopotential method. Independent-particle wave functions of core electrons vary strongly with nodes due to the strong Coulomb attraction of the nucleus and orthogonality requirement. This makes the use of plane-wave basis set impractical. However, many relevant properties of a system, e.g. bonding, chemical reactivity and response to external perturbations, are mostly related to valence electrons only. In other words, core electrons are quite inert to the act of external changes in many cases. It is therefore a good approximation to consider the core electrons and the corresponding nucleus as a rigid object. One can see core electrons as frozen in the nuclei and the sea of valence electrons in matters as moving in a background of ion cores composed of nuclei and inert core electrons. In this approximation, the effects of the nucleus and the core electrons on the valence electrons via Coulomb interaction are replaced by an effective potential, which is call pseudopotential. This potential must give nodeless pseudo wave-functions which are identical to all-electron wave functions in the region outside a given radius and smooth enough in the core region in order to be well represented by a rather small number of plane waves in practical calculations.

Most modern pseudopotentials are based on the same idea, although they can be built by different procedures. Pseudopotentials are constructed for isolated atom and then used for calculations of molecular and solid systems. First, an all-electron calculation

is performed, e.g by solving Kohn-Sham equation in a given DFT framework, for single isolated atom in order to obtain the electronic states. Then the core electron states are kept in the ground state of atomic configuration, whilst valence ones are pseudized in such a way that they are unchanged in the region outside a cut-off, and are smooth and nodeless in the region inside. The corresponding pseudopotential is found by inverting the Kohn-Sham equation. The requirement that the norm of the wave functions, i.e. their total charge, is conserved leads to the so-called *norm conserving pseudopotentials* [25]. This norm-conservation condition ensures the correct description of the atomic scattering properties around the atomic reference energy and leads to much improved results with respect to empirical pseudopotentials which are not norm-conserving.

Norm-conserving pseudopotential of elements like N, O, F and the first row of transition metals are still quite "hard"; significant amount of Fourier components are needed to have a good representations. This can be remedied in a procedure proposed by Vanderbilt called *ultrasoft* pseudopotential [26] scheme where the norm-conservation requirement can be relaxed without compromising the atomic scattering properties and the pseudopotential is chosen as smooth as possible to reduce the number of plane wave used in the expansion. The usual Kohn-Sham eigenvalue problem now becomes a generalized eigenvalue problem with the addition of an overlap operator which depends on the inonic positions. The full electron density is obtained by adding an augmentation charge, localized in the core regions, to the usual part coming from the square modulus of the orbitals as in the norm-conserving case. This approach is technically rather complicated, but it has been demonstrated to be extremely successful in practical electronic calculations.

The supercell approach for finite systems. The plane-wave pseudopotential method was originally designed for infinite periodic system like bulk crystals. In many system, such as atoms, molecules, surfaces, periodicity is not present at least in one direction. It is also natural to think that for finite systems other methods, such as the use of localized basis sets or solving KS equations directly on a real-space grid, are more appropriate. It turns out, however, that plane-wave pseudopotential method is also very useful in study-

ing systems lacking periodicity. This is done by using the so-called supercell approach. In this approach, the system is artificially repeated to form a periodic system which is suitably studied by plane-wave pseudopotential method. The supercell method should be accurate if there is enough empty space between atoms or molecules in the artificially periodic system in order to eliminate spurious interactions of the system located in a unit cell with its periodic images. The need for a large image separation means that many plane waves must be used. Nevertheless, due to the efficiency of the plane waves method this has been proven to be an effective way of solving the problem. We will use this approach together with plane-wave pseudopotential method in calculating RPA correlation energy and van der Waals coefficients for non-spherical systems (molecules) presented later.

Developments and improvements of methods, algorithms as well as computational facilities during last several decades have made DFT with plane-wave pseudopotential method become the most widely-used tool in electronic structure calculation nowadays. Plane wave pseudopotential method as briefly presented above for calculations of electronic total energy as well as many other quantities, such as, for instance phonon frequencies, infrared and Raman cross section, electron-phonon interaction coefficient, etc, has been implemented in the suite of code called QUANTUM-ESPRESSO [65].

Chapter 2

Correlation energy in the Adiabatic Connection Fluctuation-Dissipation Theory

2.1 Introduction

It has been mentioned in the previous chapter that the Local Density Approximation and the Generalized Gradient Approximations for exchange-correlation functional describe well many properties of both finite and extended systems. However, it is also well known that DFT within LDA or GGAs fails in many other cases, for instance, in strongly correlated materials and in a variety of weakly bonded compounds of which noble gas dimers and solids, layered materials, and bio-molecules are a few examples.

The limitations of LDA and GGAs in describing weakly bound systems are due to their local and semilocal nature. Nonlocal correlations, of which van der Waals forces are one manifestation, are obviously out of the scope of LDA and GGA. During the last two decades, there have been several attempts to overcome this limitation of LDA and GGA. A simple and computationally convenient way is to add to the energy obtained with traditional DFT calculations a dispersion energy contribution in the form of C_6/R^6

multiplied by an appropriate damping function that removes the divergence at zero separation of the fragments that constitute the system [27]. This approach has been applied to study many van der Waals complexes with some successes [28]. The main limitation is in its semiempirical nature; there is not a unique way to select the damping function and C_6 coefficients. There have been attempts, such as X3LYP hybrid functional [29], to construct a "standard" xc-functional being able to describe van der Waals forces, but with very limited success.

Recently, more sophisticated approaches based on the exact expression for the correlation energy given by the Adiabatic Connection Fluctuation-Dissipation (ACFD) theorem [7] have been shown to be a promising way to obtain accurate correlation energies of electronic systems. Together with very accurate treatment of the exchange energy in the DFT exact-exchange calculation, these approaches open a possibility to describe properly van der Waals systems. These applications made so far range from atomic systems [6, 14] to simple molecules [9, 10, 11, 12] and bulk solids [13, 15] with implementations based on real-space radial grid, localized basis set and plane wave pseudopotential method. This approach is however very computationally involved (even in comparison with the exact-exchange calculation which is already much more expensive than standard DFT within LDA or GGA.) This is probably the main reason why only a limited number of applications of the method have been made so far.

In the following we will derive some expressions useful for the calculation of correlation energy in the ACFD formalism. We will also present our implementation of the formalism based on the framework of Density Functional Perturbation Theory [30], starting with presentation of the formalism in a very general form, independent of the basis set. Formulae useful for practical implementation in the plane-wave pseudopotential method will then be shown together with the application to bulk silicon system serving as a testing ground. A variant of the implementation suitable for closed-shell atomic systems, where one can take advantage of spherical symmetry property to solve equations on a radial grid, will be described in the appropriated place in the following chapters.

2.2 Correlation energy in the Adiabatic Connection Fluctuation-Dissipation Theory

In this section we will re-derive the exact expression of exchange-correlation energy based on the Adiabatic-Connection Fluctuation-Dissipation Theorem (ACFDT). Let us start by considering a system consisting of N electrons interacting with each other via Coulomb interaction and moving in an external local potential $v_{ext}(\mathbf{r})$. The Hamiltonian reads

$$H = T + v_{ext} + v_{int}, \tag{2.1}$$

where T and v_{int} are the kinetic energy and non-local Coulomb operator, respectively. Let us call $n(\mathbf{r})$ the ground state electronic density and introduce fictitious systems of N electrons where Coulomb interaction between electrons is scaled by λ ($0 \leq \lambda \leq 1$) and the external potential is v_{ext}^{λ} such that the ground state density is unchanged

$$H_\lambda = T + v_{ext}^{\lambda} + \lambda v_{int}. \tag{2.2}$$

When $\lambda = 0$, these electrons are non-interacting and the corresponding auxiliary system is nothing but the Kohn-Sham system and hence $v_{ext}^{\lambda=0} = v_{KS} = v_{ext} + v_H + v_{xc}$. In the other limit, i.e. $\lambda = 1$, the interaction is the physical one hence $v_{ext}^{\lambda=1} = v_{ext}$. If we denote Ψ^λ the ground state of H_λ, then according to Hellmann-Feynman theorem

$$\frac{dE(\lambda)}{d\lambda} = \frac{d}{d\lambda}\langle\Psi^\lambda|H_\lambda|\Psi^\lambda\rangle = \langle\Psi^\lambda|v_{int}|\Psi^\lambda\rangle + \langle\Psi^\lambda|\frac{\partial v_{ext}^{\lambda}}{\partial\lambda}|\Psi^\lambda\rangle. \tag{2.3}$$

Integrating this equation over λ between 0 and 1 we obtain

$$E_{\lambda=1} = E_{\lambda=0} + \int_0^1 d\lambda\langle\Psi^\lambda|v_{int}|\Psi^\lambda\rangle + \int d\mathbf{r}\; n(\mathbf{r})[v_{ext}(\mathbf{r}) - v_{KS}(\mathbf{r})] \tag{2.4}$$

With the following decompositions of energy functional

$$E_{\lambda=1} = T_s + E_H + E_{xc} + \int v_{ext}(\mathbf{r})n(\mathbf{r})d\mathbf{r},$$

and

$$E_{\lambda=0} = T_s + \int v_{KS}(\mathbf{r})n(\mathbf{r})d\mathbf{r},$$

we get the familiar identity

$$E_H + E_{xc} = \int_0^1 d\lambda \langle \Psi^\lambda | v_{int} | \Psi^\lambda \rangle. \tag{2.5}$$

Now we will relate the integrand on the right hand side of the above equation to the density-density linear response function at imaginary frequency $\chi_\lambda(\mathbf{r}, \mathbf{r}'; iu)$. To this end, we will first prove the following identity

$$\langle \Psi^\lambda | v_{int} | \Psi^\lambda \rangle = \frac{1}{2} \int d\mathbf{r} d\mathbf{r}' \ \frac{1}{|\mathbf{r} - \mathbf{r}'|} \{ \langle \hat{n}(\mathbf{r}) \hat{n}(\mathbf{r}') \rangle_\lambda - \delta(\mathbf{r} - \mathbf{r}') \langle \hat{n}(\mathbf{r}) \rangle_\lambda \}, \tag{2.6}$$

where $\hat{n}(\mathbf{r}) = \sum_{i=1}^N \delta(\mathbf{r} - \mathbf{r}_i)$ is the number-density operator and $\langle ... \rangle_\lambda$ means average in the ground state corresponding to coupling constant λ. Indeed, we can write the left hand side as follows

$$\begin{aligned} \langle \Psi^\lambda | v_{int} | \Psi^\lambda \rangle &= \langle \Psi^\lambda | \frac{1}{2} \sum_{i \neq j} \frac{1}{|\mathbf{r}_i - \mathbf{r}_j|} | \Psi^\lambda \rangle = \frac{1}{2} \sum_{i \neq j} \int d\mathbf{r}_1 ... d\mathbf{r}_N \frac{1}{|\mathbf{r}_i - \mathbf{r}_j|} |\Psi^\lambda(\mathbf{r}_1, ..., \mathbf{r}_N)|^2 \\ &= \frac{1}{2} \int d\mathbf{r} d\mathbf{r}' \frac{1}{|\mathbf{r} - \mathbf{r}'|} n_2^\lambda(\mathbf{r}, \mathbf{r}'), \end{aligned} \tag{2.7}$$

where the pair-probability density $n_2^\lambda(\mathbf{r}, \mathbf{r}')$ is obtained by integrating $N - 2$ arbitrary variables of $|\Psi^\lambda|^2$ and then multiplying by N(N-1) (the result is the same for any set of variables because $|\Psi^\lambda|^2$ is fully symmetric due to the indistinguishability of particles). On the other hand, after inserting the definition of number-density operator, the right hand side of Eq. (2.6) becomes

$$\begin{aligned} &\frac{1}{2} \int \frac{d\mathbf{r} d\mathbf{r}'}{|\mathbf{r} - \mathbf{r}'|} \int d\mathbf{r}_1 ... d\mathbf{r}_N \left\{ \sum_{i,j=1}^N \delta(\mathbf{r} - \mathbf{r}_i) \delta(\mathbf{r}' - \mathbf{r}_j) - \delta(\mathbf{r} - \mathbf{r}') \sum_{i=1}^N \delta(\mathbf{r} - \mathbf{r}_i) \right\} |\Psi^\lambda|^2 \\ = &\frac{1}{2} \int \frac{d\mathbf{r} d\mathbf{r}'}{|\mathbf{r} - \mathbf{r}'|} \int d\mathbf{r}_1 ... d\mathbf{r}_N \left\{ \sum_{i,j \neq i}^N \delta(\mathbf{r} - \mathbf{r}_i) \delta(\mathbf{r}' - \mathbf{r}_j) + \sum_{i=1}^N \delta(\mathbf{r} - \mathbf{r}') \delta(\mathbf{r} - \mathbf{r}_i) - \right. \\ &\left. \delta(\mathbf{r} - \mathbf{r}') \sum_{i=1}^N \delta(\mathbf{r} - \mathbf{r}_i) \right\} |\Psi^\lambda|^2 \\ = &\frac{1}{2} \int \frac{d\mathbf{r} d\mathbf{r}'}{|\mathbf{r} - \mathbf{r}'|} \{ n_2^\lambda(\mathbf{r}, \mathbf{r}') + \delta(\mathbf{r} - \mathbf{r}') n(\mathbf{r}) - \delta(\mathbf{r} - \mathbf{r}') n(\mathbf{r}) \} \\ = &\frac{1}{2} \int d\mathbf{r} d\mathbf{r}' \frac{1}{|\mathbf{r} - \mathbf{r}'|} n_2^\lambda(\mathbf{r}, \mathbf{r}'). \end{aligned}$$

This is exactly the right hand side of the Eq. (2.7) and thus the identity is proven.

Next we introduce the density fluctuation operator defined by

$$\delta\hat{n}(\mathbf{r}) = \hat{n}(\mathbf{r}) - n(\mathbf{r}). \tag{2.8}$$

Putting $\hat{n} = n + \delta\hat{n}$ into the definition of the pair-probability density (by Eqs. (2.6) and (2.7)) with the note that $\langle\delta\hat{n}\rangle = 0$, we have

$$n_2^\lambda(\mathbf{r},\mathbf{r}') = \langle\Psi^\lambda|\delta\hat{n}(\mathbf{r})\delta\hat{n}(\mathbf{r}')|\Psi^\lambda\rangle + n(\mathbf{r})n(\mathbf{r}') + \delta(\mathbf{r}-\mathbf{r}')n(\mathbf{r}). \tag{2.9}$$

This equation shows that the pair-probability density can be expressed through the ground-state density and the density fluctuation (the first term on the right hand side) of the system. On the other hand, the latter can be related to the energy dissipation, i.e. the imaginary part of the density-density linear response function, of the system by the celebrated Fluctuation-Dissipation theorem, first derived in Ref. [31] and later restated in DFT framework [7]. In this context, the relation between the pair-density $n_2^\lambda(\mathbf{r},\mathbf{r}')$ and density-density response function $\chi_\lambda(\mathbf{r},\mathbf{r}';iu)$ reads[1]

$$-\int_0^\infty \frac{du}{\pi}\chi_\lambda(\mathbf{r},\mathbf{r}';iu) = n_2^\lambda(\mathbf{r},\mathbf{r}') - n(\mathbf{r})n(\mathbf{r}') + \delta(\mathbf{r}-\mathbf{r}')n(\mathbf{r}). \tag{2.10}$$

Multiplying both sides with $1/|\mathbf{r}-\mathbf{r}'|$ and integrating over $\mathbf{r},\mathbf{r}'$ and λ we obtain

$$\begin{aligned}
&-\frac{1}{2}\int_0^1 d\lambda\int d\mathbf{r}d\mathbf{r}'\frac{1}{|\mathbf{r}-\mathbf{r}'|}\left\{\int_0^\infty\frac{du}{\pi}\chi_\lambda(\mathbf{r},\mathbf{r}';iu)+\delta(\mathbf{r}-\mathbf{r}')n(\mathbf{r})\right\}\\
&=\frac{1}{2}\int_0^1 d\lambda\int d\mathbf{r}d\mathbf{r}'\frac{1}{|\mathbf{r}-\mathbf{r}'|}n_2^\lambda(\mathbf{r},\mathbf{r}')-\frac{1}{2}\int_0^1 d\lambda\int d\mathbf{r}d\mathbf{r}'\frac{n(\mathbf{r})n(\mathbf{r}')}{|\mathbf{r}-\mathbf{r}'|}\\
&=\int_0^1 d\lambda\langle\Psi^\lambda|v_{int}|\Psi^\lambda\rangle - E_H
\end{aligned} \tag{2.11}$$

Comparing with (2.5), we get an exact expression for E_{xc}

$$E_{xc} = -\frac{1}{2\pi}\int_0^1 d\lambda\int d\mathbf{r}d\mathbf{r}'\frac{1}{|\mathbf{r}-\mathbf{r}'|}\left\{\int_0^\infty\chi_\lambda(\mathbf{r},\mathbf{r}';iu)du+\delta(\mathbf{r}-\mathbf{r}')n(\mathbf{r})\right\} \tag{2.12}$$

[1]It is more convenient to use the density-density response function at an imaginary frequency since this quantity is a real and smooth (without pole) function on the imaginary axis.

It is noted that if χ_λ in this expression is replaced by χ_0 which is the density-density response function of the (non-interacting) KS electrons, having the familiar expression in term of KS orbitals, $\phi_i(\mathbf{r})$, KS eigenvalues, ϵ_i, and occupation numbers, f_i,

$$\chi_0(\mathbf{r},\mathbf{r}';iu) = \sum_{i,j}(f_i - f_j)\frac{\phi_i^*(\mathbf{r})\phi_j(\mathbf{r})\phi_j^*(\mathbf{r}')\phi_i(\mathbf{r}')}{\epsilon_i - \epsilon_j + i\hbar u}, \tag{2.13}$$

an expression similar to the one for the Hartree-Fock exchange but evaluated with the Kohn-Sham orbitals instead of the Hartree-Fock ones is obtained

$$E_x = -\frac{e^2}{2}\int d\mathbf{r}d\mathbf{r}'\frac{|\sum_i^{occ}\phi_i^*(\mathbf{r})\phi_i(\mathbf{r}')|^2}{|\mathbf{r}-\mathbf{r}'|}. \tag{2.14}$$

The exchange-correlation energy can thus be separated into the KS exchange energy, E_x, and the correlation energy, E_c. The former is represented by the Eq. (2.14) and is the counterpart of Hartree-Fock exchange energy in the context of density-functional theory. The latter, i.e. correlation energy, can be expressed in term of response functions as

$$E_c = -\frac{1}{2\pi}\int_0^1 d\lambda \int_0^\infty du\ \mathrm{Tr}\{v_c[\chi_\lambda(iu) - \chi_0(iu)]\}, \tag{2.15}$$

where the notation Tr is the trace over spatial coordinates. The interacting response χ_λ can be evaluated in the framework of time-dependent density functional theory by solving the Dyson-like equation relating χ_λ and χ_0 [32]

$$\chi_\lambda(iu) = \chi_0(iu) + \chi_0(iu)\left[\lambda v_c + f_{xc}^\lambda(iu)\right]\chi_\lambda(iu), \tag{2.16}$$

with the unknown exchange-correlation kernel $f_{xc}^\lambda(iu)$ needing to be approximated in practical applications.

2.3 Practical EXX/RPA+ scheme for exchange and correlation energies

Exchange and correlation energies calculated from equations (2.14) and (2.15) are exact provided that exact Kohn-Sham orbitals are used. In practice, the xc-functional is

not know and one can only use approximate Kohn-Sham orbitals to evaluate them. In principle, one can make a self-consistent procedure by taking functional derivatives of E_x and E_c with respect to the density to obtain exchange-correlation potential for the next iteration. In fact, the calculation of exact exchange potential can be carried out routinely at present for both molecular [33] and extended systems [34]. The evaluation of the correlation potential in the ACFD theory is however a practically formidable task; almost all of the calculations of correlation energy in this formalism made so far did not include any attempt of self-consistency. The correlation energy is evaluated using LDA, GGA, or EXX Kohn-Sham orbitals and energies as commonly done in excited state MBPT calculations [35].

Practical calculations of correlation energy in ACFD theory still need an approximation for the xc-kernel in Eq. (2.16) in order to evaluate χ_λ. The knowledge that can be used to construct a physical approximation for the xc-kernel is much less than that for the xc-functional since xc-kernel also depends on coupling constant λ and imaginary frequency iu. Several attempts have been spent on developing an approximate xc-kernel [36], but very limited improvement has been achieved. Although xc-kernel is definitely relevant in the determination of the *absolute* correlation energy of an electronic systems, it is expected, and in fact there is some evidence that the choice of xc-kernel is not very critical for evaluating structural properties [37, 38]. This is because structural properties are determined by the energy *differences* between different configurations of an isoelectronic system for which some degree of error cancellation can be expected. Nevertheless, this is still an open issue [11], and there are several attempts to find an optimal xc-kernel for correlation energy calculations [39].

Random Phase Approximation (RPA) corresponds to the simplest approximation where the xc-kernel is completely neglected and it has been known to account for long range correlation effects [7], but its description of short-range correlation is very poor [40]. The RPA correlation alone gives too large (in magnitude) correlation energy and it has been abandoned for direct use in DFT calculations a few decades ago. Quite recently, it has been proposed that the inaccuracy of RPA in the description of correlation energy

can be improved by combining RPA with a short-range correction of LDA or GGA correlations. Kurth and Perdew pointed out in Ref. [37] that the short-range correction to RPA can be done in a local approximation, while gradient-correction contribution to this correction are significantly smaller than those needed for the full correlation energy. This suggests a procedure to obtain more accurate exchange and correlation energies which has proven to describe properly several difficult systems in which long-range van der Waals energy plays a crucial role.

The practical scheme, often called EXX/RPA+, which gives more accurate xc-energy by combining the exact exchange and RPA correlation energy can be described as follows. First, a standard DFT calculation with LDA (GGA) is performed to get the ground state charge density. Then the exact exchange energy[2] defined in Eq. (2.14) and the RPA correlation energy defined in Eq. (2.15) is calculated using the DFT/LDA(GGA) charge density as input. The local density correction is also computed from this density. Finally the total energy of the system is obtained by replacing the LDA(GGA) exchange and correlation energies by the exact exchange energy and RPA correlation energy with the correction for the short-range part.

2.4 Existing implementations

As already mentioned in the Introduction, computation of correlation energy in ACDF formalism is extremely demanding for general systems where chemically bonded regions, e.g. in molecules or real solids, are fully treated in DFT calculation. In fact, the first implementations of the method addressed very simple cases, such as model jellium slabs [56], asymptotic van der Waals interaction of small atoms [6], or, with further simplification, asymptotic interaction of any neutral fragments [67]. The first implementation which includes the full treatment of chemically bonded regions only appeared quite recently by F. Furche [10]. This implementation is based on atomic orbitals and has an unfavor-

[2] Calculations of the exact-exchange energy in the present thesis will be performed as implemented in the `PWscf` code [64]. See also section 2.6.2.

able N^6 scaling with N being the size of the atomic orbital basis. Applications of this implementation were indeed limited to small atomic and molecular systems [10, 11].

Implementations based on plane-waves and pseudopotentials were developed quite recently with better scaling as the fourth power of the system size. They have been applied to study successfully several difficult systems where long-range correlation effects play a crucial role, ranging from an improved description of equilibrium cohesive energies and lattice constants of noble gas solids [15] to a successful description of very weakly bonded Beryllium dimer [12], and hexagonal boron nitride (h-BN), the layer structure isoelectronic to graphite [13]. In these implementations, one needs to solve the Kohn-Sham equation not only for occupied but also for many unoccupied orbitals in order to obtain an accurate representation of the Kohn-Sham response function from the explicit evaluation of the expression in term of occupied and empty orbitals given in Eq. (2.13). This representation is done in reciprocal space, resulting in a large memory requirement to store large matrices. Interacting response functions at any given coupling constant, λ, and imaginary frequency, iu, are then calculated by solving the Dyson-like equation (2.16) which now becomes a linear equation relating full matrices. CPU time and memory requirements of these calculations increase rapidly with kinetic energy cut-off, i.e. with the number of plane waves used to represent the response function. It has been observed that correlation energy converges slowly with respect to the cut-off energy. It is therefore unpractical to apply the strategy of standard DFT calculation to get converged result, namely increasing the cut-off energy until convergence. Practical calculations of the correlation energy are usually performed for an energy cut-off as small as possible and then an extrapolation scheme is used to get the correlation energy in the limit of infinite cut-off energy [13, 15]. Integrations over interaction strength, λ, and imaginary frequency, iu, can be done efficiently by the Gauss-Legendre method since correlation energies are smooth function of these variables.

There are several disadvantages in these implementations. First, the full spectrum, or at least a good part of the conduction states of the Kohn-Sham Hamiltonian is needed to represent the non-interacting response function. This prevents one from using efficient

iterative diagonalization techniques. Second, storing large matrices and solving linear equation relating them are memory-demanding and cpu-time-intensive operations that limit the size of the systems that can be treated. Finally, there is no easy way to do the λ-integration even in the case of random phase approximation where analytic results are available. In the next section, we will introduce our implementation which can overcome some of these shortcomings.

2.5 New implementation: iterative diagonalization of dielectric function

2.5.1 General formulation

In our implementation, the traces in the exact formula for the correlation energy from the ACFD theory, Eq. (2.15), are evaluated by summing up the eigenvalues of $v_c\chi_0$ and $v_c\chi_\lambda$. A number of eigenvalues of these two operators are obtained by explicit diagonalization. In principle, every eigenvalue contributes to the correlation energy and one would need to calculate the whole spectrum of these operators whose size equals the number of plane waves in the basis set.

Band structure calculations of the inverse RPA dielectric matrix [57] for several bulk crystals have shown however that only a small fraction of the spectrum differs significantly from 1; all the rest approaches 1 quite rapidly. As RPA dielectric function, ϵ_{RPA}, is simply related to $v_c\chi_0$ by

$$\epsilon_{RPA} = 1 - v_c\chi_0, \tag{2.17}$$

this means that only a small fraction of the spectrum of $v_c\chi_0$ differs significantly from zero; the remaining eigenvalues will be close to zero. Also, very recent calculations for several silicon nanostructures confirm this behavior [58]. Therefore correlation energy can be obtained accurately (at least this is expected for correlation-energy *differences* if not for *absolute* values) calculating only a limited number of low-lying eigenvalues ($v_c\chi_0$ is a negative definite operator) which give significant contribution to the correlation energy;

the contribution from the remaining part of the spectrum can be reduced to an arbitrarily small value by increasing the number of the calculated eigenvalues or can be approximated, for instance, by a model as done for the calculation of electronic band gap in the Ref. [59].

In our implementation of ACFD formulas we focus on RPA, i.e neglecting the xc-kernel in Eq. (2.16). In this approximation eigenvalues of $v_c\chi_\lambda$ are related to those of $v_c\chi_0$ by a simple relation, thus allowing an analytical evaluation of the λ-integration. To show this relationship, let us start by introducing the following two generalized eigenvalue problems for $v_c\chi_0$ and $v_c\chi_\lambda$

$$\chi_0|w_\alpha\rangle = a_\alpha v_c^{-1}|w_\alpha\rangle, \tag{2.18}$$

$$\chi_\lambda|z_\alpha^\lambda\rangle = b_\alpha^\lambda v_c^{-1}|z_\alpha^\lambda\rangle, \tag{2.19}$$

where $\{a_\alpha, |w_\alpha\rangle\}$ and $\{b_\alpha, |z_\alpha^\lambda\rangle\}$ are the eigenpairs of the two eigenvalue problems, respectively. Once the sets of $\{a_\alpha\}$ and $\{b_\alpha^\lambda\}$ are known, the correlation energy contribution for a given interaction strength λ can be calculated as

$$E_c^\lambda = -\frac{1}{2\pi}\int_0^\infty du \sum_\alpha \left\{b_\alpha^\lambda(iu) - a_\alpha(iu)\right\}. \tag{2.20}$$

Since the xc-kernel is set to zero in RPA, the Dyson-like equation, Eq. (2.16) becomes simply

$$\chi_\lambda = \chi_0 + \lambda\chi_0 v_c \chi_\lambda. \tag{2.21}$$

Response functions and Coulomb operator are negative and positive definite quantities respectively, they are invertible[3] and the above equation can be written in the form

$$\chi_0^{-1} = \chi_\lambda^{-1} + \lambda v_c. \tag{2.22}$$

Therefore when the xc-kernel is approximated in RPA, there is a simple relation between b_α^λ and a_α which enable us to compute correlation energy from $\{a_\alpha\}$ only. To see

[3] Both χ_0 and χ_λ (and v_c^{-1}) have a zero eigenvalue corresponding to a uniform perturbing potential. Beside this "trivial" solution, whose contribution can be calculated analyzing the limit for slowly varying potentials, the stability of the system implies that χ_0 and χ_λ are negative definite quantities.

this, let us write the eigenvalue problems of Eq. (2.18) and (2.19) in the equivalent forms

$$\chi_0^{-1}|w_\alpha\rangle = \frac{1}{a_\alpha} v_c|w_\alpha\rangle, \tag{2.23}$$

and

$$\chi_\lambda^{-1}|z_\alpha^\lambda\rangle = \frac{1}{b_\alpha^\lambda} v_c|z_\alpha^\lambda\rangle. \tag{2.24}$$

Using the relation (2.22) between χ_λ and χ_0 together with Eqs. (2.23) and (2.24), one can see that χ_λ and χ_0 have the *same set of eigenfunctions*, i.e. $z_\alpha^\lambda \equiv w_\alpha$ and their eigenvalues are simply related as

$$b_\alpha^\lambda = \frac{a_\alpha}{1 - \lambda a_\alpha}. \tag{2.25}$$

The integration over λ can therefore be done analytically and we obtain the final expression for E_c in term of eigenvalues $\{a_\alpha\}$ of the non-interacting problem alone

$$E_c = \frac{1}{2\pi} \int_0^\infty du \ \sum_\alpha \{a_\alpha(iu) + \ln(1 - a_\alpha(iu))\}. \tag{2.26}$$

This expression means that knowing the eigenvalues of the problem defined by Eq. (2.18) is sufficient to compute the correlation energy E_c.

In order to determine the needed eigenvalues we proceed by solving iteratively the eigenvalue problem (2.18). To this end we implemented a variant of the Davidson diagonalization used in the solution of the KS equation, but any other iterative diagonalization scheme could also be used. The basic operation involved in any iterative diagonalization routine is the one where the response function χ_0 is applied to some trial perturbing potential. The result of this action is the linear density response which can be computed efficiently in the same way as in the calculation of vibrational properties with the well-established techniques of Density Functional Perturbation Theory [30]. Note that the density response we need to calculate here is that of the non-interacting system, thus there is no need of performing a self-consistent cycle as instead is needed in the actual DFPT calculations of the density response to the screened perturbing potential. This makes the calculation of a single density response used in the iterative diagonalization procedure cheaper than that of other calculations, such as, for instance, phonon frequencies. However several iterations, i.e. several applications of χ_0 to trail potentials, are

needed to obtain well-converged eigenvalues. This makes the computational cost of the two calculations for a given system become more or less similar.

In summary, following the approach discussed above one can avoid the need of computing a large number of unoccupied Kohn-Sham orbitals as well as cumbersome summations over occupied and unoccupied states. Valence states of the Kohn-Sham Hamiltonian and low-lying eigenvalues of the generalized eigenvalue problem (2.18) needed for evaluation of the correlation energy can be computed efficiently by iterative-diagonalization technique. We wish to mention that a similar idea has been used very recently by Wilson and co-workers as presented in Ref. [58] but for the calculation of static dielectric properties of several silicon nanostructures.

2.5.2 New implementation in plane wave pseudopotential approach

The formulation of our method for the calculation of RPA correlation energy presented in the previous section is very general and in principle applies to all cases. More detail of the implementation for applications to systems with spherical symmetry will be discussed later in the appropriate place. In this section, we will present some technical aspects of the implementation in the plane-wave pseudopotential method based on the `phonon` code which is part of the QUANTUM-ESPRESSO distribution [65].

In the plane wave pseudopotential approach, a system is treated as periodic although it can be aperiodic or partially periodic, e.g. isolated molecules, polymer chains and slabs. As a consequence of this periodicity, the dielectric function in plane-wave representation is block diagonal and can be classified by a vector $\mathbf{q}$ in the first Brillouin zone. Its eigenpotentials can be chosen as Bloch's waves with the same $\mathbf{q}$-vector. Therefore one can evaluate the correlation energy by diagonalizing separately the generalized eigenvalue problem (2.18) for each block to compute the contribution at a given $\mathbf{q}$-vector. The total correlation energy is then obtained by integration over the first Brillouin zone. As a result

of this, expression (2.15) for the correlation energy can be written as

$$E_c = -\frac{1}{2\pi}\int_0^1 d\lambda \int_0^\infty du\ \frac{1}{N_q}\sum_{q=1}^{N_q} \mathrm{Tr}\{v_c[\chi_\lambda(\mathbf{q},iu) - \chi_0(\mathbf{q},iu)]\}. \tag{2.27}$$

The corresponding expression in the case of RPA, Eq. (2.26), becomes

$$E_c = \frac{1}{2\pi}\int_0^\infty du\ \frac{1}{N_q}\sum_{q=1}^{N_q}\sum_{\alpha}^{N_{eig}} \{a_\alpha(\mathbf{q},iu) + \ln(1 - a_\alpha(\mathbf{q},iu))\}, \tag{2.28}$$

where $a_\alpha(\mathbf{q},iu)$ is an eigenvalue of the generalized eigenvalue problem (2.18) for $\chi_0(\mathbf{q})$.

In practice, the sum over a regular grid of $\mathbf{q}$-vectors in the first Brillouin zone can be reduced by making use of the special point technique [60]. This is because, like in the case of electronic band structures, the eigenvalues of $v_c\chi_0$ at equivalent $\mathbf{q}$-vectors, i.e. those transformed to each other by a symmetry operation of the system, are equal. Unlike the case of electronic band structure, special care must be taken when doing the calculation in the limit of $\mathbf{q} \to 0$ because of the non-analyticity of dielectric function at $\mathbf{q} = 0$. In other words, the generalized eigenvalue problem (2.18) for the case of $\chi_0(\mathbf{q} = 0)$ is ill-defined. We have not found any better solution to overcome this problem than simply avoiding the point $\mathbf{q} = 0$ by using a shifted grid of $\mathbf{q}$-vectors in the special point technique.[4]

In our implementation, we will calculate low-lying eigenvalues $a_\alpha(\mathbf{q},iu)$ of the non-interacting problem in Eq. (2.18) by using a variant of the Davidson iterative diagonalization algorithm for dealing with the generalized eigenvalues problem starting from a set of (random) trial eigenpotentials. The basic operation involved in this (or any other iterative diagonalization scheme) is the application of the non-interacting χ_0 to a trial potential to obtain the induced density response. This can be done by resorting to the linear response techniques of Density Functional Perturbation Theory [30], simply generalized to imaginary frequency as already explained below[5]. Similar techniques were introduces

[4] This point was not mentioned in other plane wave pseudopotential implementations [12, 13, 15] but it is likely that the same strategy could also have been adopted in these implementations.

[5] A general derivation of the equation to determine the density response starting from the expression of non-interacting linear response function (2.13) will be given in the Appendix A.

by Mahan [52, 54] for the calculation of frequency dependent polarizabilities of atomic systems.

Let us consider the following eigenvalue problem for an electron in a periodic solid within the independent particle approximation

$$\hat{H}_{SCF}(\mathbf{r})\varphi^0_{\mathbf{k},v}(\mathbf{r}) = \varepsilon_{\mathbf{k},v}\varphi^0_{\mathbf{k},v}(\mathbf{r}), \tag{2.29}$$

where $\hat{H}_{SCF}$ is a time-independent Hamiltonian. Time dependence of the wave function is simply given by a phase factor

$$\psi^0_{\mathbf{k},v}(\mathbf{r},t) = \varphi^0_{\mathbf{k},v}(\mathbf{r})e^{-i\varepsilon_{\mathbf{k},v}t}. \tag{2.30}$$

The application of the non-interacting response function to a trial potential, needed to be done routinely in the iterative diagonalization procedure, gives the density response defined by

$$\Delta n(\mathbf{r};iu) = \int \chi_0(\mathbf{r},\mathbf{r}';iu)\Delta V(\mathbf{r}';iu)d\mathbf{r}' \tag{2.31}$$

For given **q**-vector, this imaginary-frequency density-response can be computed efficiently using the linear response technique of Density Functional Perturbation Theory by considering the following time-dependent perturbation potential added to the Hamiltonian $\hat{H}_{SCF}(\mathbf{r})$

$$\Delta V(\mathbf{r},t) = \left[\Delta v(\mathbf{r})e^{i\mathbf{qr}} + \Delta v(\mathbf{r})^* e^{-i\mathbf{qr}}\right] e^{ut}, \tag{2.32}$$

with $\Delta v(\mathbf{r})$ being a lattice-periodic potential. Under this perturbation, the ground state wave function $\psi^0_{\mathbf{k},v}(\mathbf{r},t)$ changes to $\psi_{\mathbf{k},v}(\mathbf{r},t)$ which can always be decomposed as

$$\psi_{\mathbf{k},v}(\mathbf{r},t) = \psi^0_{\mathbf{k},v}(\mathbf{r},t) + \Delta\psi_{\mathbf{k},v}(\mathbf{r},t). \tag{2.33}$$

where $\Delta\psi_{\mathbf{k},v}(\mathbf{r},t)$ can be written in the form

$$\Delta\psi_{\mathbf{k},v}(\mathbf{r},t) = \left[\Delta\varphi^+_{\mathbf{k},v}(\mathbf{r})e^{i\mathbf{qr}} + \Delta\varphi^-_{\mathbf{k},v}(\mathbf{r})e^{-i\mathbf{qr}}\right] e^{-i\varepsilon_{\mathbf{k},v}t}e^{ut}. \tag{2.34}$$

The corresponding density response induced by the perturbation is simply

$$\begin{aligned}\Delta\tilde{n}(\mathbf{r},t) &= \sum_{\mathbf{k},v}\left\{\psi^0_{\mathbf{k},v}(\mathbf{r},t)^*\Delta\psi_{\mathbf{k},v}(\mathbf{r},t) + \psi^0_{\mathbf{k},v}(\mathbf{r},t)\Delta\psi_{\mathbf{k},v}(\mathbf{r},t)^*\right\} \\ &= \sum_{\mathbf{k},v}\left\{\left[\varphi^0_{\mathbf{k},v}(\mathbf{r})^*\Delta\varphi^+_{\mathbf{k},v}(\mathbf{r}) + \varphi^0_{\mathbf{k},v}(\mathbf{r})\Delta\varphi^-_{\mathbf{k},v}(\mathbf{r})^*\right] e^{i\mathbf{qr}} + c.c.\right\} e^{ut},\end{aligned} \tag{2.35}$$

or in a compact form

$$\Delta\tilde{n}(\mathbf{r}, iu) = \left\{\Delta n(\mathbf{r})e^{i\mathbf{qr}} + \Delta n(\mathbf{r})^* e^{-i\mathbf{qr}}\right\}, \tag{2.36}$$

with

$$\Delta n(\mathbf{r}) = \sum_{\mathbf{k},v} \left\{\varphi^0_{\mathbf{k},v}(\mathbf{r})^* \Delta\varphi^+_{\mathbf{k},v}(\mathbf{r}) + \varphi^0_{\mathbf{k},v}(\mathbf{r})\Delta\varphi^-_{\mathbf{k},v}(\mathbf{r})^*\right\} \tag{2.37}$$

(frequency dependence is implicitly implied.)

Linear density response can be obtained from variations of the wave functions $\varphi^+_{\mathbf{k},v}(\mathbf{r})$ and $\varphi^-_{\mathbf{k},v}(\mathbf{r})$ keeping only first-order terms of the perturbation expansion. Equations to determine them can be derived by inserting the expression of $\psi_{\mathbf{k},v}(\mathbf{r}, t)$ in Eq. (2.33) into the time-dependent Schrödinger's equation that must be fulfilled

$$\left(\hat{H}_{SCF}(\mathbf{r}) + \Delta V(\mathbf{r}, t)\right) \psi_{\mathbf{k},v}(\mathbf{r}, t) = i\frac{\partial}{\partial t}\psi_{\mathbf{k},v}(\mathbf{r}, t), \tag{2.38}$$

and keeping only the linear order terms. We obtain

$$\left(\hat{H}_{SCF}(\mathbf{r}) - \varepsilon_{\mathbf{k},v} - iu\right) \Delta\psi_{\mathbf{k},v}(\mathbf{r}, t) = -\Delta V(\mathbf{r}, t)\psi^0_{\mathbf{k},v}(\mathbf{r}, t) \tag{2.39}$$

Using the explicit expression of $\psi_{\mathbf{k},v}(\mathbf{r}, t)$ in Eq. (2.34), we find the following two equation for $\varphi^+_{\mathbf{k},v}(\mathbf{r})$ and $\varphi^-_{\mathbf{k},v}(\mathbf{r})$

$$\left(\hat{H}_{SCF}(\mathbf{r}) - \varepsilon_{\mathbf{k},v} - iu\right) \varphi^+_{\mathbf{k},v}(\mathbf{r}) = -\Delta v(\mathbf{r})\psi^0_{\mathbf{k},v}(\mathbf{r}) \tag{2.40}$$

$$\left(\hat{H}_{SCF}(\mathbf{r}) - \varepsilon_{\mathbf{k},v} - iu\right) \varphi^-_{\mathbf{k},v}(\mathbf{r}) = -\Delta v(\mathbf{r})^*\psi^0_{\mathbf{k},v}(\mathbf{r}). \tag{2.41}$$

Solving these equation at a finite value of iu is no more complex than the case of $iu = 0$, typically occurring for calculation of phonon frequencies. The only difference is that for the latter the operator on the left hand side is Hermitian, hence methods for solving linear systems like conjugate gradient apply directly. For the former, the operator is no longer Hermitian due to the appearance of iu, thus one needs to use a more general algorithm to deal with non-Hermitian linear systems, e.g. biconjugate gradient [24] or minimal residual [61]. We have chosen however to use the efficient bi-CGSTAB algorithm invented by H. van der Vorst in 1992 [62] since this algorithm is the most stable with

better convergence rate among several ones that we have tried. We have also found that the higher the imaginary frequency iu, the faster the convergence of the linear system. Therefore, computational workload at finite iu is not more than that of the static case.

Now we turn to the discussion of the efficiency of our implementation in comparison with the other plane-wave pseudopotential implementations of ACFD formalism whose most involved operations are *i)* the construction the noninteracting Kohn-Sham response function χ_0 in Eq. (2.13) by making summation over occupied and empty states and *ii)* the solution of the Dyson-like equation relating χ_0 and χ_λ. Since some general aspects of the similar method have already been discussed in Ref. [58], we will limit the discussion here to the points related to the calculation of RPA correlation energy. In a plane wave representation, the set-up of non-interacting response function by summation over valence and conduction bands scales like $N^2_{pw\chi_0} N_v N_c$, where $N_{pw\chi_0}$ is the size of the basis set used to represent χ_0, and N_v, N_c are the number of valence and conduction states used in the sum, respectively. The most time-consumming part in our implementation is the calculation of the linear density response via DFPT. This calculation takes a time propotional to $N_{pw\psi} N_v^2$ with $N_{pw\psi}$ being the number of plane wave used to represent the wave function (typically smaller than $N_{pw\chi_0}$ by an order of magnitude.) Since this calculation is done repeatedly in the iterative diagonalization procedure, the total computational cost must be multiplied by the number of eigenvalues (N_{eig}) we want to calculate and the number of iterations N_{iter}. The latter is independent of the system size while the former is easily propotional to it. Therefore the total scaling of this approach is propotional to $N_{pw\psi} N_v^2 N_{eig}$ which grows as the fourth power of the system size, i.e. the same as those of other plane wave implementations.

Although the scaling of our implementation is not better than those of other plane wave implementations, its pre-factor is much smaller, at least of the order of 10^2, making our implementation more efficient. To see this in detail, let us recall that in general $N_v \ll N_{pw\psi} \ll N_{pw\chi_0}$ and the relative scaling of the former and the latter is $N_{iter} \frac{N_{pw\psi}.N_{eig}.N_v.N_v}{N_{pw\chi_0}.N_{pw\chi_0}.N_v.N_c}$. Since $\frac{N_{pw\chi_0}}{N_{pw\psi}} \sim 10$, $\frac{N_{pw\chi_0}}{N_{eig}} \sim 10 \div 100$ (as can be seen in the next section), $\frac{N_c}{N_v} \sim 10$, and the number of iterations in iterative diagonalization procedure N_{iter} is not more than 10,

the pre-factor in our implementation is $10^2 \div 10^3$ smaller.

Moreover, it is easy to see that our approach also has significant advantages due to its iterative nature. Eigenvalues and eigenvectors of the generalized eigenvalue problem (2.18) will converge very rapidly if the initial guess of the eigenpotentials is close to the real ones. It is reasonably to expect that the form of eigenpotentials of a system will not dramatically change if some parameters to determine them, e.g. k-point sampling or the basis set, are varied. This suggest a procedure that may save considerable CPU time by first doing the calculation with looser convergence parameters, then using the obtained results as the starting trial-vectors for more refined calculations. Since the calculation of correlation energy requires the computation of eigenvalues on a grid of $\mathbf{q}$-vectors, eigenpotentials calculated at a vector $\mathbf{q}$ are also a good guess at $\mathbf{q}+\Delta\mathbf{q}$ with small $\Delta\mathbf{q}$. Similar behavior can be also observed looking at the problem at iu and $iu + \delta iu$ which is needed to be solved for integration over imaginary frequency. Finally, as already mentioned in the general formulation, coupling constant integration in our implementation is completely avoided and this also saves a lot of computational time.

2.5.3 Testing and improving numerical efficiency of the implementation

In order to validate the implementation described above, we have chosen to reproduce some results appeared in literature. First of all, we compared our results for some top eigenvalues of RPA dielectric function of eight-atom bulk silicon simple-cubic cell with those calculated by explicit diagonalization of the dielectric matrix and by Projective Dielectric EigenPotential method which is a scheme very similar to ours which has been very recently described in Ref. [58]. Table 2.1 presents top 20 eigenvalues of dielectric matrix calculated by two methods discussed in the Ref. [58] and those obtained from our implementation. Calculation was done using norm-conserving pseudopotentials [66] at $\mathbf{q} = 0.01$ in the z-direction with the kinetic energy cut-off of 12 Rydberg and a cubic cell of 10.20 bohr size length. Iterative diagonalization procedure was terminated when the

Index	RPA	PDEP	Ours	Index	RPA	PDEP	Ours
1	14.7432	14.7538	14.7611	11	2.4910	2.4925	2.4925
2	3.4231	3.4237	3.4238	12	2.4905	2.4920	2.4920
3	3.3908	3.3914	3.3915	13	2.4905	2.4920	2.4920
4	3.3908	3.3914	3.3915	14	2.4716	2.4721	2.4721
5	3.3908	3.3914	3.3915	15	2.1964	2.1972	2.1972
6	3.3908	3.3914	3.3915	16	2.1960	2.1968	2.1968
7	3.3589	3.3596	3.3596	17	2.1959	2.1966	2.1967
8	2.4910	2.4925	2.4925	18	2.1959	2.1966	2.1967
9	2.4910	2.4925	2.4925	19	2.1958	2.1966	2.1967
10	2.4910	2.4925	2.4925	20	2.1958	2.1966	2.1967

Table 2.1: Top 20 eigenvalues of dielectric matrix for the eight-atom bulk silicon cubic cell. RPA: from direct evaluation of diagonalization of the dielectric matrix. PDEP: from similar method proposed in the Ref. [58]. Ours: from calculation in our implementation.

differences between eigenvalues at successive iterations were less than 10^{-5} Rydberg. The table shows clearly that there is an excellent agreement between our calculated values and those obtained from a similar method but in different implementation[6], and both results are also in good agreement with the result obtained by direct diagonalization of the dielectric matrix. As already mentioned in Ref. [58], lower-lying eigenvalues were also found to be close although those of RPA direct method are highly sensitive to the number of empty states used in the calculation of the dielectric matrix.

Next, we performed calculations of total energies for bulk silicon, hence lattice constant in EXX/RPA+, with correlation energies treated in the EXX/RPA+ scheme. Note that the same calculations have been done by García-González and co-workers as shown in Ref. [13], where due to the very large computational cost calculations were not fully converged

[6]This implementation makes use of the method of orthogonal iteration with Ritz acceleration which requires twice applications of the linear response function to a set trial potentials at each iteration step.

and some extrapolation technique was needed to make the calculations feasible. We have chosen these calculation to be the reference for checking the validity of our implementation.

Bulk silicon is a typical covalently bond solid and many properties, such as, for instance, structural and vibrational properties, are described satisfactorily in DFT within LDA. One can anticipate that the difference between LDA and EXX/RPA+ results will be marginal. Nevertheless, the calculation will be illustrative since, as pointed out in Ref. [13], the results demonstrate well the error cancellation between exchange and correlation energies in LDA. Moreover, the calculation also illustrates the robustness of EXX/RPA+ method, namely not only does it give better description of systems where long-range correlation plays an important role, but also preserves the LDA or GGA already satisfactory description of densely-packed systems. From the computational point of view, it is useful to perform calculations on system with moderate computational expenses like bulk silicon in order to collect data for developing an extrapolation schemes to improve numerical efficiency of this approach.

For systems with dispersive electronic levels like bulk silicon, the most important parameters whose convergence needs to be carefully checked in the calculation are the number of $\mathbf{k}$ points in the standard LDA calculation for the ground state charge density, the number of $\mathbf{q}$ points used in the evaluation of Eq. (2.27) and the number of plane waves, i.e. kinetic-energy cutoff, used in the representation of quantities like wave functions, charge density, potential, etc. Specifically to our implementation, there is another important parameter determining efficiency of the approach: the number of eigenvalues needed to evaluate correlation energy from Eq. (2.28).

First of all, let us investigate the convergence of the correlation energy with respect to the number of eigenvalues included in the summation of Eq. (2.26). For this purpose, we have used well-converged parameters for standard LDA calculation of silicon ground state charge density to evaluate the exact-exchange and RPA-correlation energies. Namely, the calculation was performed for the diamond structure in the fundamental face-centered cubic with lattice constant of 10.20 bohr (corresponding to the equilibrium geometry at LDA level) using a regular grid of 64 k-point, a kinetic-energy cut-off of 20 Rydberg,

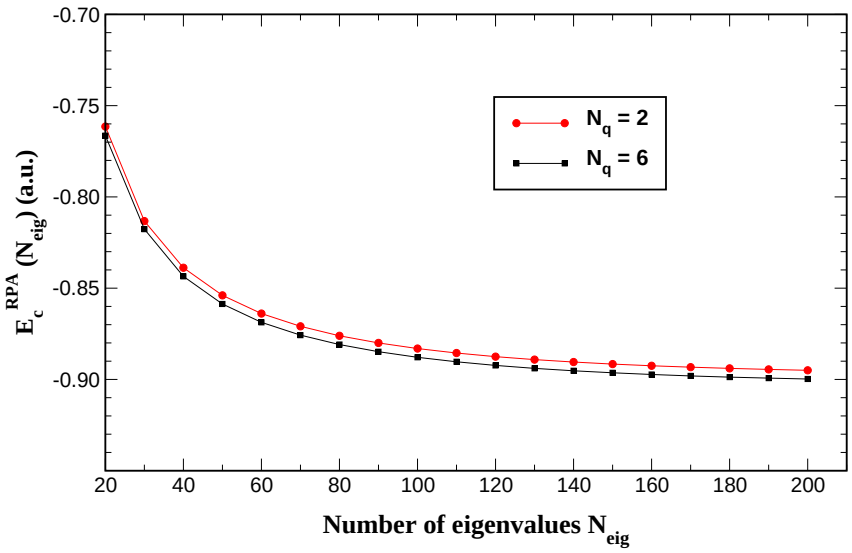

Figure 2.1: RPA correlation energy as function of the number of eigenvalues included in the summation in Eq. (2.26) for fcc bulk silicon. The two curves are for different number of special $\mathbf{q}$ points in the Brillouin zone integration of Eq. (2.28).

and the same pseudopotential used for the calculation of the top most eigenvalues of the dielectric function of the eight-atom bulk silicon cubic cell presented above. We show in Fig. (2.1) the dependence of RPA correlation energy, E_c^{RPA}, on the number of eigenvalues included in the sum N_{eig}. E_c^{RPA} is indeed a rapidly converging function of N_{eig}; truncating the sum at 80 or 100 eigenvalues already ensures a convergence within a few mRy. Also the summation over special $\mathbf{q}$-point representing the integration in the first Brillouin zone converges very rapidly; the correlation energy changes only a few mRy when the number of special points increases from 2 to 6.

We have also calculated total energies of bulk silicon at different lattice constants in the EXX/RPA+ scheme in order to determine its equilibrium properties, i.e. the lattice constant and the bulk modulus. Fig. 2.2 shows the total energy per unit cell for bulk silicon as function of lattice constant (the value at experimental lattice constant is subtracted) calculated using different values N_{eig} ($N_{eig} = 50, 100, 150$ and 200) for the number of eigenvalues included in the summation in Eq. (2.26) in our implementation for the EXX/RPA+ scheme. The (nearly) coincidence of the different curves confirms the

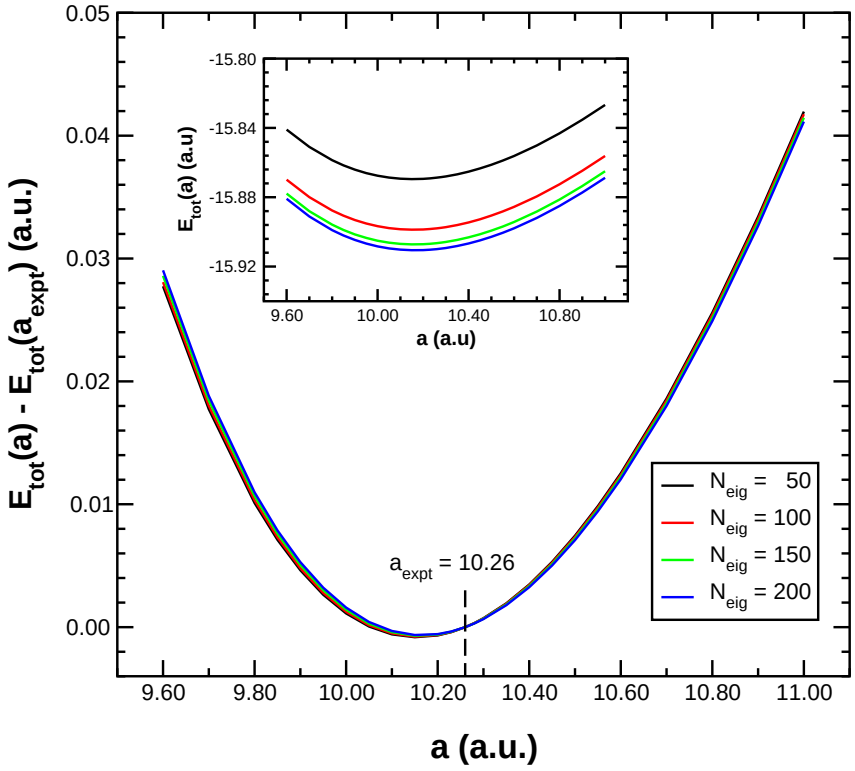

Figure 2.2: The total energy (per unit cell) differences at different lattice constants and that at the experimental one of bulk silicon calculated using different number of eigenvalues values included in the summation in Eq. (2.26) in our implementation of EXX/RPA+ scheme. The inset is the true total energy. i.e. the values at the experimental lattice constant is not subtracted.

expectation that energy differences are rather insensitive to the number of eigenvalues, N_{eig}, used in the calculation of the RPA correlation energy. This is because, as clearly seen in the inset where the true EXX/RPA+ total energy are shown, the curves calculated with increasing values of N_{eig} are almost rigidly shifted downward.

Table 2.2 shows the predicted equilibrium lattice parameter a_0, bulk modulus B and pressure derivative of the bulk modulus B' as a function of the number of eigenvalues N_{eig} used to evaluate RPA correlation energies. The differences of these quantities when changing N_{eig} from 50 to 200 is very small, of the order of 0.1% for a_0 and B and 1% for B'. We can therefore conclude that only a relatively small number of eigenvalues used for

N_{eig}	a_0 (a.u.)	B (GPa)	B'
50	10.155	99.5	4.22
100	10.158	99.4	4.21
150	10.162	99.3	4.19
200	10.166	99.1	4.17
LDA	10.235	92.5	4.16
Expt[†]	10.26	99.2	4.15

[†] Experimental data are taken from Ref. [63]

Table 2.2: Predicted equilibrium lattice parameter a_0, bulk modulus B and pressure derivative of the bulk modulus B' as function of the number of eigenvalues N_{eig} used to evaluate RPA correlation energies. The corresponding LDA and experimental values are also shown in bottom rows.

the evaluation of RPA correlation energy in our implementation of the ACFD formalism is needed to get a good description of many equilibrium properties of the system.

On the other hand, looking at the predicted equilibrium lattice constants in table 2.2, it seems that more accurate (and sophisticated) treatment of xc-energy in EXX/RPA+ scheme slightly worsens the LDA results compared to the experimental values. Nevertheless, as pointed out in Ref. [13], there are several points that can affect the final results: (i) EXX/RPA+ scheme is not self-consistent and the RPA correlation energy is evaluated using LDA Kohn-Sham orbitals, (ii) RPA is the simplest approximation to the xc-kernel within ACFD formalism, and (iii) EXX/RPA+ scheme here is implemented in a pseudopotential approximation. Possible influences of these points to the final results were also discussed in Ref. [13].

It is worth mentioning that when looking at the exchange and correlation energies separately, our results also show the well-known cancellation of errors in these two quantities in the standard DFT/LDA calculation as already presented in Ref. [13]. Namely, when

compared with the more accurate values obtained in EXX/RPA+ scheme, the (absolute) LDA exchange-energy underestimates the EXX one while the opposite behavior is found for the correlation energy. These two errors compensate each other leading to practically the same values for the total LDA and EXX/RPA+ xc-energies.

Let us now turn to the discussion of the convergence of RPA correlation energy with respect to other parameters. Slow convergence of the *absolute* RPA correlation energy in ACFD formalism as implemented in a plane-wave pseudopotential approach with kinetic-energy cutoff has been observed in other implementations [13, 15], and efficient extrapolation schemes were needed to get the correlation energy at infinite value of energy cut-off. Since our implementation here is also in the plane-wave pseudopotential approach, these extrapolation schemes can be easily adapted to fit the same purpose. For the convergence with respect to the Brillouin zone integration, both for $\mathbf{k}$ point used for the calculation of ground state charge density which is then used as input for the calculation of RPA correlation energy and $\mathbf{q}$ point used for evaluation of the correlation energy itself from Eq. (2.28), we have carefully analyzed the data and have found that the dependence of E_c^{RPA} on these parameters is very well-behaved.

For instance, in Fig. 2.3 we plot in each panel the difference between RPA correlation energy calculated using a coarser grid of special $\mathbf{q}$ points generated using Monkhorst-Pack recipe [60] and the value calculated using the very accurate grid of $6 \times 6 \times 6$ ($N_q = 28$) as function of the kinetic-energy cutoff. Note that the value obtained by $6 \times 6 \times 6$-grid is well-converged since the difference between the results of this grid and the $5 \times 5 \times 5$ one (the bottom panel) is of the order of less than one mRy. The figure shows clearly that the differences of E_c^{RPA} calculated using a coarser grid of $\mathbf{q}$ vectors and the well-converged value obtained from a denser grid are *almost unchanged with respect to the kinetic-energy cutoff* once the cutoff is larger than a certain, but not very large, value ($12 - 16$ Ry.) A similar behavior was also observed when keeping fixed the number of $\mathbf{q}$ points and varying the number of $\mathbf{k}$ points. This suggests an extrapolation scheme similar to the one proposed in Ref. [13] which can help reducing significantly the computational effort in large systems for which even the present very efficient implementation is too demanding

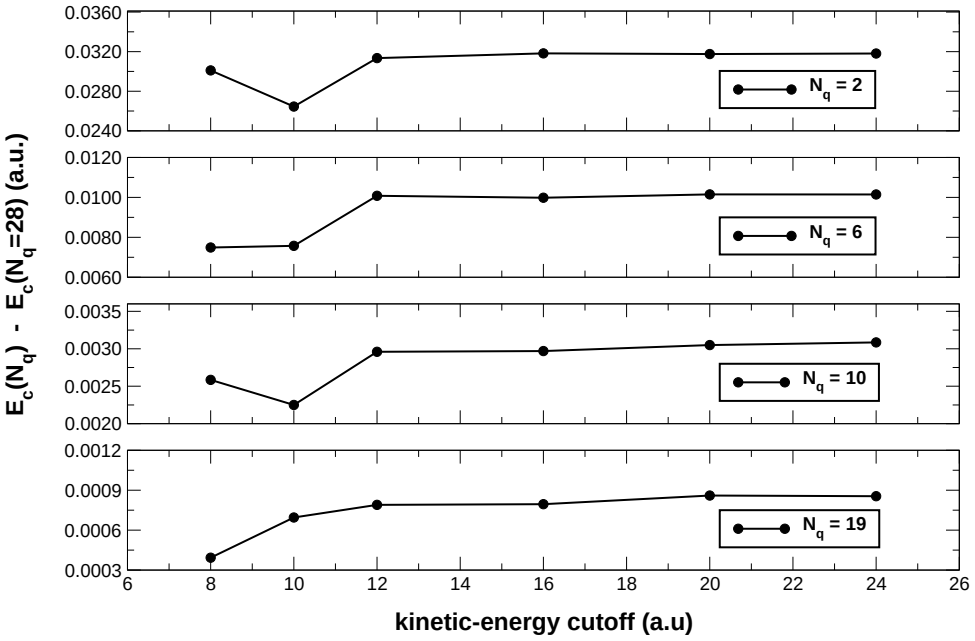

Figure 2.3: The differences between RPA correlation energy calculated at a small number of special $\mathbf{q}$ points, N_q, and that at well-converged values $N_q = 28$ as function of kinetic-energy cutoff.

to reach complete convergence directly. The procedure can be described as follows: First a coarse grid of $\mathbf{k}$- and $\mathbf{q}$-points for the Brillouin zone integration is used to calculate RPA correlation-energy at different kinetic-energy cutoffs. Second, the correlation energy in the infinite cutoff limit is obtained by extrapolating the results obtained at finite cutoffs. Finally, the errors due to the coarse $\mathbf{k}$- and $\mathbf{q}$-point sampling of Brillouin zone are corrected by using finer grids evaluated at small kinetic-energy cutoff (which can be estimated from the convergence behavior of the correlation energy computed with the coarser grids.)

2.6 EXX/RPA+ description of the Beryllium dimer

2.6.1 Previous DFT studies of Beryllium dimer

Beryllium dimer is one example of weakly bonded systems where standard DFT within LDA or GGA performs poorly. The first DFT study of Be_2 in the plane wave pseudopo-

tential method with a supercell approach for the description of isolated molecules was probably performed by Richardson and co-workers more than two decades ago [69]. In this study, the LDA result for the bond length of the molecule was 4.53 bohr which is quite in good agreement with the experimental value of 4.63 bohr. LDA predicts however a too large binding energy, four times larger in absolute value (0.43 eV) than the experimental one (0.098 eV). The ground-state vibrational frequency of 373 cm^{-1} also seriously overestimates the experimental value of 275.8 cm^{-1}. Later developed GGA functionals, while giving a value of bond length closer to experiment, do not improve much the LDA results for the binding energy and vibrational frequency (see, e.g. the recent calculations reported in Ref. [12].)

Ground state properties of Be_2 molecule have been re-investigated recently by Fuchs and Gonze [12] in the ACFD approach with a plane-wave pseudopotential implementation. In this study, the binding energy, bond length, and vibrational frequency have been calculated using different approximations for the xc-kernel in Eq. 2.16, namely RPA and the more sophisticated orbital-dependent PGG kernel [36]. Equilibrium properties of Be_2 molecule is then determined from the total energies as a function of interatomic distance calculated in much the same way as in the EXX/RPA+ scheme presented above, but the short-range correction for RPA correlation energy is not included in the EXX/RPA scheme, and the correlation energy is calculated with PGG-kernel in the EXX/PGG one. The results of all three schemes improve much LDA and GGA descriptions of the ground-state properties of Be_2 demonstrating the ability of ACFD approach to describe weakly bound systems. This calculation is however numerically still not very accurate as the quoted convergence error in the binding energy calculation is about as large as 50%. Beside serving as another testing ground for our implementation of ACFD approach, Be_2 will also demonstrate that very accurate treatments of both exact-exchange and RPA(+) correlation energies is indeed needed in order to get well-converged results. It is very important to have accurate calculations since the quality of RPA approximate xc-kernel, and hence the EXX/RPA(+) scheme, is usually drawn from its performance when applied to study real systems and this evaluation should not be contaminated by numerical or

convergence errors.

2.6.2 Controlling numerical accuracy of the exact-exchange and RPA correlation energies in our implementation

In our calculation, we used the same norm-conserving pseudopotential as in Ref. [12] which was generated from a free-atom calculation within exact Kohn-Sham exchange. Since the supercell approach is used to simulate an isolated molecule, we have to carefully check the convergence with respect to the following parameters: kinetic-energy cutoff, size of the supercell, and the number of eigenvalues used for evaluation of the RPA correlation energy.

First of all, it is natural to estimate the values of the kinetic-energy cutoff and the size of the supercell that should give converged results in EXX/RPA+ scheme by performing some convergence tests at the LDA level. As for the kinetic-energy cutoff, we found that with a given simple-cubic supercell of 22 bohr, increasing the cutoff from 25 to 30 Ry makes the total energies of Be_2 change by less than 0.5 mRy at a number of Be-Be

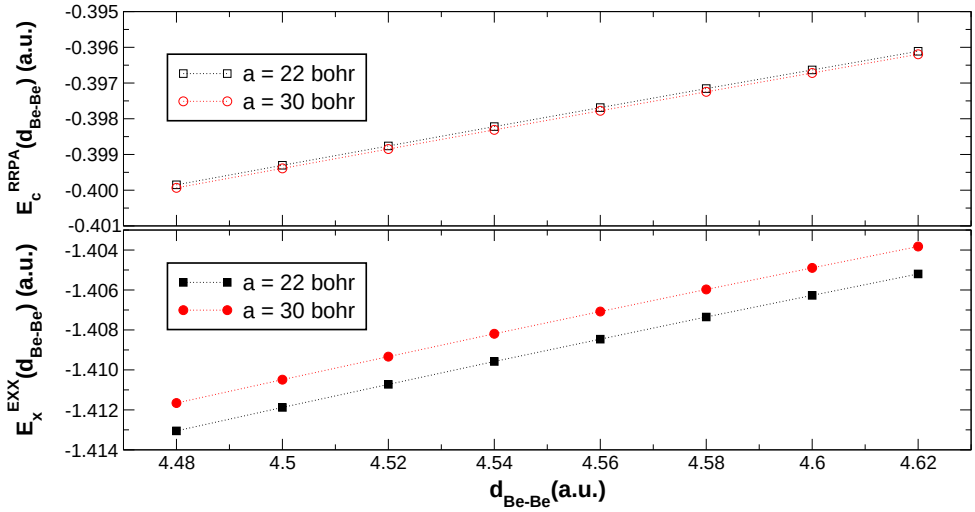

Figure 2.4: Exact-exchange and RPA correlation energies of Be_2 at different Be-Be distances (d_{Be-Be}) calculated using a simple cubic cell size lengths of 22 (square) and 30 (circle) bohr. The dotted lines are simply drawn as a guide.

distances around the LDA predicted equilibrium value. This suggests that a kinetic-energy cutoff of 25 Ry will also give well-converged results for exact-exchange and RPA correlation energies. Our explicit calculations confirm that this is in fact the case: the energy change of the exact exchange energy between 25 and 30 Ry is of the same order as the total energy differences mentioned above while it is an order of magnitude smaller for the case of RPA correlation energy.

Convergence with respect to the size of supercell is much more delicate as shown in Fig 2.4 where we plot the exact-exchange and RPA correlation energies as a function of the distance between two Be atoms. While the LDA total energies (not shown) and RPA correlation energies are only slightly changed (of the order of 0.1 mRy, see the top panel of Fig. 2.4) when the size of the simulation cell increases from 22 to 30 bohr, the differences of the exact-exchange energies is at least one order of magnitude larger than this value for all Be-Be distances (see the bottom panel). Slow convergence of the exact-exchange as implemented in a plane-wave pseudopotential method with respect to the Brillouin zone sampling has been known for a long time [70] (see also Refs. [13] and [15]). This is because in a plane-wave representation, the expression for exchange energy contains an integrable divergence which prevents the direct application of the special-point technique. The problem is usually circumvented by using a procedure originally developed by Gygi and Baldereschi [70] where a reference term with the same singularity is subtracted to remove the divergence. It is possible to choose the reference term in such a way that its integration in the Brillouin zone can be done analytically. By this device the divergence is removed and the special-point technique can be applied. However, there is still a term which remains non-divergent in the limit of $\mathbf{q} \to 0$ but can not be computed at $\mathbf{q} = 0$ since it is a 0/0 limit [71]. If this term is simply neglected (as usually the case) one makes an error proportional to $1/(\Omega N_k)$, where Ω and N_k are the volume of the unit cell and the number of special $\mathbf{k}$ points used for representation of the Brillouin sampling, respectively. From the computational point of view, it is convenient to use a number of $\mathbf{k}$ points as small as possible and, in the supercell approach, to use a simulation cell with small volume. Therefore the error in the exact-exchange energy by neglecting the limiting

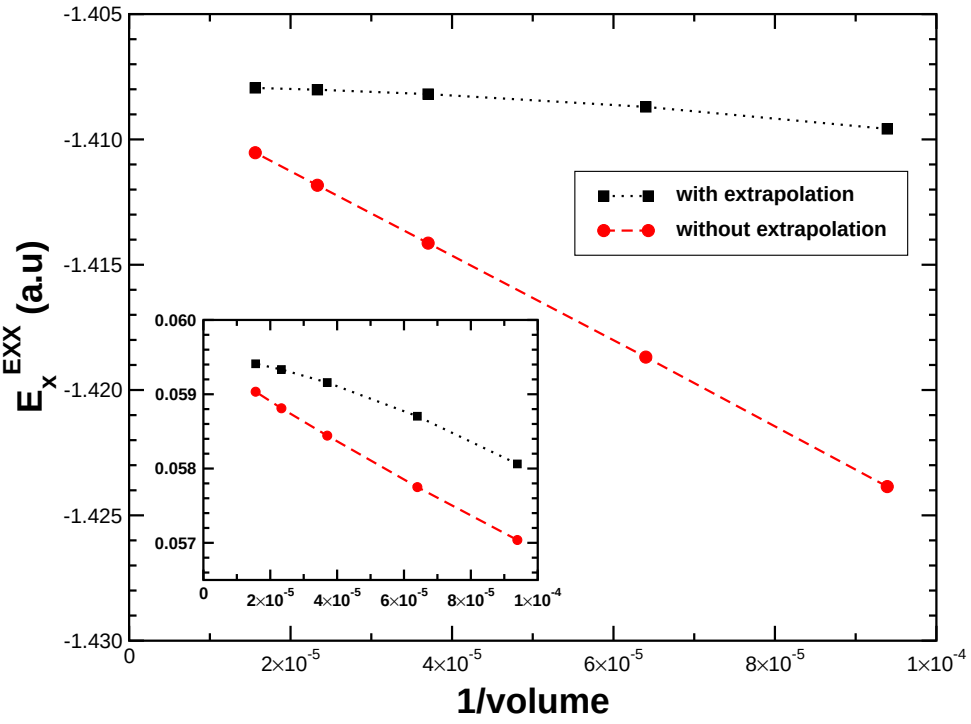

Figure 2.5: Exact-exchange energies as function of supercell volume for Be_2 at the Be-Be distance of 4.54 bohr calculated with (square) and without (circle) extrapolation scheme. Inset: The same quantities but subtracted twice the exact-exchange energy of a single Be atom simulated in the same supercell. The dashed and dotted line are simply drawn as a guide.

term may be large.

This problem can be partly alleviated by using an extrapolation scheme to extract an estimate of the limiting term [71]. The scheme is based on the assumption that the grid of points used for Brillouin zone integration is dense enough so that a coarser grid formed by keeping only half of the **k**-points in each direction also gives the same result for the integral. Since the number of point in the denser grid is 8 time larger than that of the coarser one, the estimated value of the limiting term is given by the difference of 8/7 times the value of the integral in the denser grid and 1/7 times that of the coarser one. This extrapolation scheme has been implemented in the `PWscf` code [64] which is part of the QUANTUM-ESPRESSO distribution [65]. We show in Fig. 2.5 a comparison

of the convergence with respect to the volume of the supercell for Be_2 at Be-Be distance of 4.54 bohr using simple cubic cells with size length of $22, 25, 30, 35$ and 40 bohr. The figure shows clearly that neglecting the limiting term, i.e. without extrapolation, there is a large error inversely proportional to the supercell volume since the E_x^{EXX} energy plotted as a function of the inverse volume is almost on a straight line. Moreover, the convergence in this case is rather slow; when the size of the supercell increases from 22 to 40 bohr, the value of E_x^{EXX} varies more than 10 mRy. On the contrary, its change is of the order of the mRy if the extrapolation scheme is exploited, demonstrating the efficiency of the scheme[7]. Note that some degree of error cancellation can also be expected when calculating the energy difference with the reference system (single Be atom in this case) which presumably makes the convergence rate faster even without using the extrapolation scheme. However, as shown in the inset in Fig. 2.5 where these energy differences are plotted, the errors at 22 bohr are still large, more than 1 mRy (with extrapolation) and 2 mRy (without extrapolation). The error decreases rapidly to a few tenth of mRy for the former while it still more than 1 mRy for the latter at 30 bohr supercell. Due to this slow convergence of the exact exchange, one needs to be very careful in order to have accurate results (less than 1 mRy) in the EXX/RPA(+) scheme.

Finally, in order to investigate the convergence with respect to the number of potential eigenvalues included in the summation of Eq. (2.28), we plot in Fig. 2.6 the RPA correlation energies of Be_2 calculated at a number of Be-Be distances (d_{Be-Be}) around the predicted bond length, using different number of eigenvalues N_{eig} for evaluation of Eq. (2.28). We are fully confident that a convergence within 0.5 mRy for the *absolute* correlation energy can be obtained using a N_{eig} as large as 220 because the figure shows clearly that energy differences between $N_{eig} = 180$ and $N_{eig} = 220$ are less than this value.

[7]We have also checked the convergence with respect to the $\mathbf{k}$ point integration for the case of Argon solid calculated using LDA wave-functions. In this case, using a regular grid of $6 \times 6 \times 6$ points is enough for a convergence of the order of 0.1 mRy (less than 2 meV), while in a similar calculation recently reported in Ref. [15], not including any correction for the $\mathbf{q} \to 0$ limit, a much denser grid of $12 \times 12 \times 12$ points must be used in order to reach this accuracy.

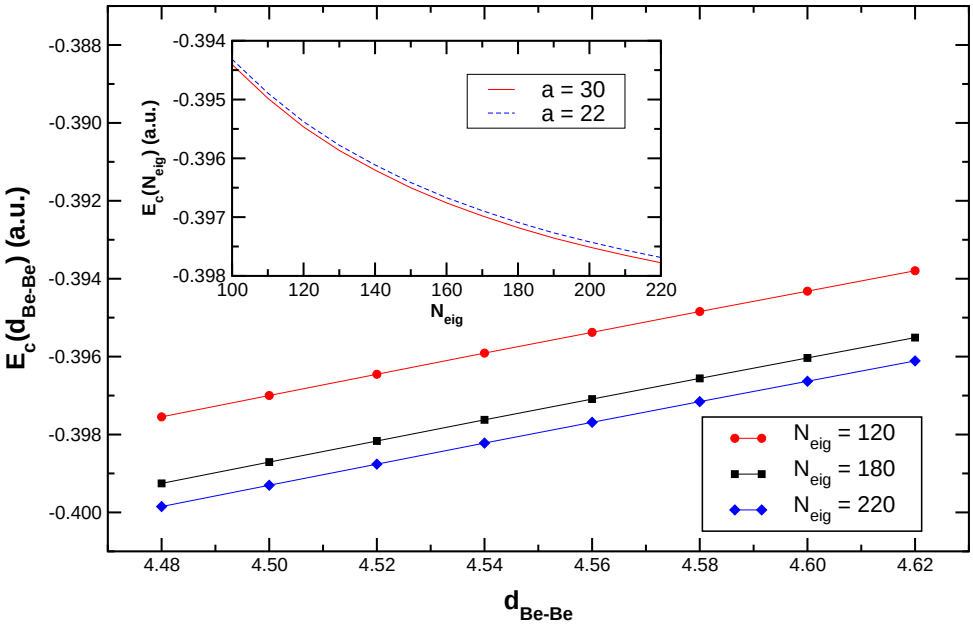

Figure 2.6: RPA correlation energies of Be_2 at different Be-Be distances (d_{Be-Be}). The curves are for different number of eigenvalues N_{eig} included for evaluation of Eq. (2.28): $N = 120$ (circle), $N = 180$ (square), and $N = 220$ (diamond). The lines are simply drawn as a guide. Inset: RPA correlation energies of Be_2 at the Be-Be distance (d_{Be-Be}) of 4.56 bohr placed in a simple cubic supercell with the size length of 22 (blue dashed line) and 30 bohr (red solid line).

This can also be seen in the inset where RPA correlation energy of Be_2 at $d_{Be-Be} = 4.56$ bohr as a function of N_{eig} is plotted. Note that one can expect a much smaller error of the correlation-energy *differences* which actually determine equilibrium properties like bond length or binding energy. The inset also shows that a fully converged result for the correlation energy can be obtained using a simple-cubic supercell with a size of 22 bohr as the change is negligible when using a larger cell of 30.

2.6.3 Equilibrium properties of Beryllium dimer studied in the EXX/RPA+ scheme

Having reached a good control of accuracy with respect to all parameters as discussed in the previous section, let us now present our results for Beryllium dimer studied in the EXX/RPA+ scheme. Table 2.3 shows binding energies, bond lengths, and vibrational frequencies of Be_2 calculated in EXX/RPA and EXX/RPA+ schemes as a function of the kinetic-energy cutoff, E_{cut}, and the number of eigenvalues, N_{eig}, used for the evaluation of RPA correlation energy. Let us first discuss the effect of changing kinetic-energies cutoff on the equilibrium properties. Increasing the kinetic-energy cutoff from 25 to 30 Ry makes a negligible change in the results for both schemes (less than 0.5% for binding energy, practically unchanged for bond length, and 1% for vibrational frequency.) When the number of eigenvalues N_{eig} is increased from the value of 120 to 220, the variations for all quantities are of the same order. Although N_{eig} needs to be as large as 220 in order to ensure that the *absolute* correlation energy convergence is less than 1 mRy, including only about half of that number is enough to get fully converged results of the interesting structural quantities which are actually determined by energy *differences*. This behavior is not totally unexpected as already discussed in chapter 2 for the case of bulk silicon. For the sake of comparison with the results by Fuchs and Gonze, we have used the parameters as similar as possible to what they used (it is impossible to choose them to be identical due to some technical differences between the two implementations). When comparing the results of $E_{cut} = 25$ Ry, whose computational parameters are closest to those used in Ref. [12], we found that our results for the absolute value of the binding energy (0.065 vs 0.08 eV in EXX/RPA scheme and 0.036 vs 0.06 eV in EXX/RPA+ one), the bond length (4.52 vs 4.52 bohr and 4.56 vs 4.59 bohr, respectively), and the vibrational frequency (297 vs 311 cm$^-$1 and 298 vs 298 cm$^-$1, respectively) are almost always smaller. Although the results of the two calculations are still in agreement within the large error bar of 0.03 eV as quoted for the binding energy in the calculation by Fuchs and Gonze (notice also that the binding energy in EXX/RPA+ in Ref. [12] is just twice this value), we see this

E_{cut}(Ry)	N_{eig}	E_b(eV)		d_0(bohr)		ω_e(cm^{-1})	
		EXX/RPA	EXX/RPA+	EXX/RPA	EXX/RPA+	EXX/RPA	EXX/RPA+
25	60	-0.0667	-0.0377	4.516	4.553	296.1	298.5
	120	-0.0657	-0.0368	4.521	4.558	296.6	298.7
	180	-0.0655	-0.0367	4.523	4.560	296.3	299.2
	220	-0.0654	-0.0365	4.524	4.561	297.1	298.5
30	60	-0.0667	-0.0376	4.515	4.551	300.0	300.4
	120	-0.0658	-0.0368	4.520	4.556	300.5	301.5
	180	-0.0658	-0.0368	4.521	4.557	300.4	301.5
	220	-0.0657	-0.0368	4.522	4.558	299.8	301.7

Table 2.3: Binding energy, bond length, and vibrational frequency of Be_2 calculated in EXX/RPA and EXX/RPA+ schemes as function of the kinetic-energy cutoff, E_{cut}, and the number of eigenvalues, N_{eig}, used for evaluation of RPA correlation energy.

as a systematic difference which deserves to be carefully studied. It turns out that the differences largely come from the exchange energy. When we used the value for the exact-exchange energy calculated without extrapolation technique, we obtained much closer values for the binding energy: -0.080 eV for EXX/RPA and -0.050 eV for EXX/RPA+ compared to -0.08 eV and -0.06 eV in Ref. [12], respectively. Note that the short-range correction for RPA+ correlation energy is not uniquely defined; using different definitions, e.g. including the gradient correction or not, would lead to slightly different results. We thus attribute the difference of our result for the binding energy in EXX/RPA+ scheme with respect to the result obtained by Fuchs and Gonze in part to this reason.

As carefully discussed when investigating the numerical accuracy of our calculations, the convergence of exact exchange energy with respect to the size of the supercell, hence the binding energy at EXX/RPA(+) level, is rather slow which is at variance with the behavior of RPA correlation energy (as well as for the total energy at the LDA level). This leads to a slow convergence of the total energies in the EXX/RPA(+) scheme.

For instance, at the kinetic-energy cutoff of 25 Ry and $N_{eig} = 220$, EXX/RPA and EXX/RPA+ schemes give the a binding energy of $-0.065(-0.037)$, $-0.059(-0.030)$, and $-0.054(-0.025)$ eV with supercells of 22, 25 and 30 bohr, respectively. From Fig. 2.5 we are confident that the exact-exchange energy calculated with our extrapolation scheme is converged at 30 bohr within 1 mRy. Therefore, our accurate calculations show that while EXX/RPA(+) schemes definitely improve the poor performance of LDA or GGA for weakly bound systems like Be_2 molecule, their results may not be as good as suggested in Ref. [12]. Therefore, the performance of RPA xc-kernel in ACFD formalism to describe real weakly bound systems still needs to be carefully investigated.

Chapter 3

Approximate response functions by Thomas-Fermi-von Weizsäcker theory

3.1 The Thomas-Fermi approximation

Thomas-Fermi method for calculating electronic structure of atomic systems [20, 21] was probably the first theory using charge density to describe the total energy of a system. In this most rudimentary form of modern DFT, electrons are treated as independent particles. The electron-electron interaction energy only comes from the classical Hartree interaction. Moreover, the kinetic energy of interacting electrons is approximated by applying locally the expression for the homogeneous non-interacting electron gas. The total energy as a functional of electron density $n(\mathbf{r})$ is thus given by

$$E[n] = \int t[n(\mathbf{r})]d\mathbf{r} + \frac{e^2}{2}\int \frac{n(\mathbf{r})n(\mathbf{r}')}{|\mathbf{r}-\mathbf{r}'|}d\mathbf{r}d\mathbf{r}' + \int V_{ext}(\mathbf{r})n(\mathbf{r})d\mathbf{r}, \tag{3.1}$$

where $t[n_0]$ is the kinetic energy density of the non-interacting homogeneous electron gas with density n_0

$$t[n_0] = \frac{3\hbar^2}{10m}(3\pi^2)^{2/3}n_0^{5/3}. \tag{3.2}$$

The electronic density in this approximation is found by minimizing the energy functional $E[n]$ in (3.1), subjected to the condition that the number of electrons is kept fixed

$$\int n(\mathbf{r})d\mathbf{r} = N \tag{3.3}$$

Using the method of Lagrange multipliers, the corresponding Euler equation, which is the well-known Thomas-Fermi equation, is obtained

$$\frac{5}{3}c_k n(\mathbf{r})^{2/3} + e^2 \int d\mathbf{r}' \frac{n(\mathbf{r}')}{|\mathbf{r} - \mathbf{r}'|} + V_{ext}(\mathbf{r}) - \mu = 0, \tag{3.4}$$

where c_k is used to denote $\frac{3\hbar^2}{10m}(3\pi^2)^{2/3}$ and μ is the Lagrange multiplier which is connected to the chemical potential.

Apparently, Thomas-Fermi approximation of kinetic energy is good for systems with slowly varying density where an electron at given point $\mathbf{r}$ sees an essentially homogeneous medium with density $n(\mathbf{r})$ around it. This is the main reason, besides the lack of proper treatment of exchange-correlation effects, why only moderate successes have been achieved when applying the method to study atoms and molecules, limited to qualitatively correct behaviors of charge density and electrostatic potential. An infinite charge density at the nucleus, a power low decaying instead of exponentially vanishing charge density in the region far from the nucleus, the lack of shell structure in describing atoms, and the inability to describe chemical binding are probably the most serious defects of the Thomas-Fermi approximation. Many improvements of this theory had been proposed and, in the next section, we will focus on the one proposed by von Weizsäcker in the 1930s, quite soon after the original work by Thomas (1927) and Fermi (1928).

3.2 An improvement of Thomas-Fermi theory: the von Weizsäcker correction

The Thomas-Fermi theory fails when a rapidly varying density occurs. In an attempt to overcome this problem, von Weizsäcker improved the approximation of the kinetic part by

introducing a correction related to the gradient of the density. The kinetic energy density in Thomas-Fermi approximation plus von Weizsäcker correction reads

$$t[n(\mathbf{r})] = \frac{3\hbar^2}{10m}(3\pi^2)^{2/3}n(\mathbf{r})^{5/3} + \frac{\hbar^2}{2m}\frac{\gamma}{4}\frac{|\nabla n(\mathbf{r})|^2}{n(\mathbf{r})}, \tag{3.5}$$

where γ is the parameter determining the contribution of the von Weizsäcker gradient-correction to the kinetic energy. The value of $\gamma = 1$ was empirically used in the original work [45].

The von Weizsäcker correction term was introduced by using intuitive and semiclassical arguments. Other attempts to improve the Thomas-Fermi approximation using density gradient expansion, focussing on systems possessing slowly varying density, obtained a lowest-order correction with the same functional form as the one proposed by von Weizsäcker, with a coefficient γ reduced by a factor of 9. Using this new coefficient in self-consistent calculation did not, however, always give better results and this reduced value of γ leads to unsatisfactorily low energies for atoms [47] and unimpressive performance in predicting other atomic properties [48]. As a consequence, empirical values of γ were usually chosen by varying between $\frac{1}{9}$ and 1 so that the results calculated in the theory best fit with experiment data.

Moreover, for the case of non-interacting electron gas, the two special values of the gradient-correction coefficient, γ, mentioned above reproduce the correct behavior of the response function in the limit of slowly and rapidly varying external perturbations as pointed out by Jones and Young in Ref. [49]. In particular, the authors compared the response function of uniform electron gas obtained by von Weizsäcker method for general γ with that of the non-interacting electron gas in the limits of small and large wave lengths. For an uniform electron gas of density n, Thomas - Fermi - von Weizsäcker method gives the response function

$$F_{TFvW}(\mathbf{q}) = -\frac{k_F}{\pi^2}\frac{1}{1+3\gamma\eta^2} \qquad \eta = \frac{q}{2k_F}, \tag{3.6}$$

with $k_F = (3\pi^2 n)^{1/3}$ being the Fermi wave vector.

The asymptotic behaviors of $F_{TFvW}(\mathbf{q})$ are

$$F_{TFvW}(\mathbf{q}) = \begin{cases} -\frac{k_F}{\pi^2}(1 - 3\gamma\eta^2 + ...) & \text{small } q \\ \\ -\frac{k_F}{\pi^2}\frac{1}{3\gamma\eta^2} & \text{large } q \end{cases} \tag{3.7}$$

On the other hand, the exact response function of the non-interacting electron gas is the well-known Lindhard's function

$$F(\mathbf{q}) = -\frac{k_F}{\pi^2}\left\{\frac{1}{2} + \frac{1-\eta^2}{4\eta} ln\left|\frac{1+\eta}{1-\eta}\right|\right\} \tag{3.8}$$

which behaves asymptotically like

$$F(\mathbf{q}) = \begin{cases} -\frac{k_F}{\pi^2}(1 - \frac{\eta^2}{3} + ...) & \text{small } q \\ \\ -\frac{k_F}{\pi^2}\frac{1}{3\eta^2} & \text{large } q \end{cases} \tag{3.9}$$

Comparing these two response functions, it is clear that the value $\gamma = 1/9$ in the von Weizsäcker correction term is the choice for slowly varying external potentials. This is the value obtained in the gradient expansion approach. On the contrary, the original value $\gamma = 1$ used by von Weizsäcker, which is not the gradient expansion result, is appropriate for rapidly varying perturbations. And, as thoroughly discussed in the Section 5.5 of Ref. [50], there is evidence that the von Weizsäcker functional is the exact kinetic energy functional in the limit of rapidly varying densities. As for this point, it is worth mentioning the interesting property that the von Weizsäcker correction term gives the exact kinetic energy in those regions of space where only one wave function is relevant. This means that the approximation will be essentially exact in the tail region of atoms and molecules where the density is small and determined by one wave function only. Moreover, electrons in the tail region are loosely-bound to nuclei, thus contribute the dominant part to the polarization of the whole system. The Thomas-Fermi approximation with the von Weizsäcker correction is therefore expected to capture essential polarization properties of finite systems like atoms and molecules.

The long-range van der Waals interaction in the asymptotic region has a close relation with the polarization properties of the system. As discussed above, the tail region is

described better with the value of $\gamma = 1$. We will use this value of γ, i.e. the original von Weizsäcker correction, when applying the approximation to calculate polarizabilities of atoms and molecules. The sensitivity of the final results on the value of γ will be also checked (and found to be small). On the other hand, we will find that the value of the full correlation energy is more sensitive to the value of γ and we will carefully study this dependence.

3.3 Approximate linear density response by TFvW functional

In order to understand the physical properties of a system, one usually acts on it with some external probe and see the change of physical quantities. In the context of Density Functional Theory, a quantity of great interest is the change of electronic density under the action of a perturbation. This is because, from the principles of DFT, any quantity can be calculated once the electronic density is given. The density response $\Delta n(\mathbf{r})$ in the linear response regime can be obtained by solving a type of modified Sternheimer [52] (for atomic systems) or DFPT [30] (for periodic systems) equations which defines the change of wave functions under an external perturbation. Since these equations involve all the ground-state wave-functions that give contributions to the charge density, the computational workload becomes very demanding when one deals with a large system. The calculation of correlation energy as described previously in Chapter 2 becomes even more demanding since one has to repeat the calculation of the linear density response to different external perturbations many times in the process of diagonalizing the response functions. Therefore, it is worth investigating the possibility of making an approximation for this kind of calculation which reduces significantly the computational workload while still keeping the accuracy to an acceptable level. In the following, we will describe one such possibility based on the the TFvW approximate kinetic energy functional.

In the context of Thomas-Fermi and von Weizsäcker approximation, it is convenient

to introduce an auxiliary wave function $\varphi(\mathbf{r})$ related to the density as

$$n(\mathbf{r}) = N|\varphi(\mathbf{r})|^2, \tag{3.10}$$

where N is the number of electrons and $\varphi(\mathbf{r})$ satisfies the normalization condition

$$\int d\mathbf{r}|\varphi(\mathbf{r})|^2 = 1. \tag{3.11}$$

The total energy functional in the Thomas-Fermi and von Weizsäcker approximation can thus be expressed in term of $\varphi(\mathbf{r})$ as

$$E[\varphi] = \frac{3\hbar^2}{10m}(3\pi^2)^{2/3}\int [N\varphi(\mathbf{r})]^{5/3}d\mathbf{r} + \frac{N\hbar^2}{2m}\gamma\int |\nabla\varphi(\mathbf{r})|^2 d\mathbf{r} + E_H[\varphi(\mathbf{r})]$$
$$+ \quad E_{xc}[\varphi(\mathbf{r})] + E_{ext}[\varphi(\mathbf{r})] - N\mu\left[\int |\varphi(\mathbf{r})|^2 d\mathbf{r} - 1\right], \tag{3.12}$$

where $E_H[\varphi(\mathbf{r})]$ and $E_{ext}[\varphi(\mathbf{r})]$ are the Hartree and external potential energies, respectively,

$$E_H[\varphi(\mathbf{r})] = \frac{e^2}{2}\int \frac{n(\mathbf{r})n(\mathbf{r}')}{|\mathbf{r}-\mathbf{r}'|}d\mathbf{r}d\mathbf{r}', \tag{3.13}$$

$$E_{ext}[\varphi(\mathbf{r})] = \int V_{ext}(\mathbf{r})n(\mathbf{r})d\mathbf{r}, \tag{3.14}$$

$E_{xc}[\varphi(\mathbf{r})]$ is the exchange-correlation energy which is approximated by LDA or some kinds of GGA, and μ is the chemical potential (Lagrange multiplier).
The self-consistent ground-state density $n(\mathbf{r})$, and hence $\varphi(\mathbf{r})$, minimizes the energy functional (3.12). From the minimization condition

$$\frac{\delta E[\varphi]}{\delta\varphi} = 0, \tag{3.15}$$

the equation determining $\varphi(\mathbf{r})$ is derived

$$-\gamma\frac{\hbar^2}{2m}\nabla^2\varphi(\mathbf{r}) + \left[V_{ext}(\mathbf{r}) + V_H(\mathbf{r}) + v_{xc}(\mathbf{r}) + \frac{\hbar^2}{2m}k_F^2(\mathbf{r})\right]\varphi(\mathbf{r}) = \mu\varphi(\mathbf{r}). \tag{3.16}$$

For a given $V_{ext}(\mathbf{r})$, self-consistent solution of this equation gives the ground-state density in the Thomas-Fermi and von Weizsäcker approximation. In fact, the equation above has been used for an approximate solution of the electronic structure problem of atoms

and molecules long before the advent of Kohn-Sham density functional theory. Electron densities for atomic systems obtained by this method exhibit the correct asymptotic behavior, decaying exponentially instead of decreasing as $1/r^6$ in the Thomas-Fermi model. Electron densities also remain finite at the nuclear position at variance with the infinite charge density obtained if the gradient correction is not included. The shell structure, however, is still missing in TFvW model, and the charge density cannot be considered very accurate.

It is important to notice here that we are not interested in obtaining the electronic ground-state density from TFvW method as much more accurate charge density can be obtained by solving the Kohn-Sham equation in LDA or GGA. Rather we are interested in calculating an approximation to the response function. It is well known that TFvW approximation give rather accurate estimate for the non-interacting kinetic energy when accurate charge densities are used while gives poor results when used to determined self-consistently the ground-state density. On a similar ground it can be hoped that also response functions (that are related to functional derivatives of the kinetic energy) are better behaved when evaluated for an accurate density. Indeed we have verified that the calculation of TFvW response function on inaccurate self-consistently determined TFvW densities leads to very poor results while the use of accurate densities leads to reasonably accurate ones.

In order to impose the desired unperturbed density distribution in the calculation of the response function it is convenient to denote the term inside square brackets in equation (3.16) by $V_{eff}(\mathbf{r})$ which can be formally obtained from $\varphi(\mathbf{r}) = \sqrt{n(\mathbf{r})}$ as

$$V_{eff}(\mathbf{r}) - \mu = \gamma \frac{\hbar^2}{2m} \frac{\nabla^2 \varphi(\mathbf{r})}{\varphi(\mathbf{r})}. \tag{3.17}$$

In principle, $V_{eff}(\mathbf{r})$ is defined from this equation once $\varphi(\mathbf{r})$ is given. For practical reasons it is not always straightforward to apply this definition in regions of low density where numerical inaccuracy in the value of $\varphi(\mathbf{r})$ may induced a noisy $V_{eff}(\mathbf{r})$. While in systems with spherical symmetry this is not very problematic since one can easily enforce the known asymptotic behavior of $V_{eff}(\mathbf{r})$ beyond a still safe radial value, for non spherical

systems expanded in plane waves the problem is more serious and some regularization procedure is needed. This procedure will be briefly outlined at the end of this chapter, let us assume for the moment that $V_{eff}(\mathbf{r})$ has been defined.

Under a small perturbation, e.g an uniform electric field, all the quantities in Eq. (3.16) deviate by a small amount from their unperturbed values. For instance, $\varphi(\mathbf{r})$ becomes $\varphi(\mathbf{r}) + \Delta\varphi(\mathbf{r})$, $n(\mathbf{r})$ becomes $n(\mathbf{r}) + \Delta n(\mathbf{r})$, etc. If only the linear order terms are considered, the variations of these quantities satisfy the following set of self-consistent equations

$$\Delta n(\mathbf{r}) = 2N\mathcal{R}e[\varphi^*(\mathbf{r})\Delta\varphi(\mathbf{r})], \tag{3.18}$$

$$\Delta V_{eff}(\mathbf{r}) = \Delta V_{ext}(\mathbf{r}) + \Delta V_H(\mathbf{r}) + \Delta v_{xc}(\mathbf{r}) + \frac{\hbar^2}{3m}\frac{k_F^2(\mathbf{r})}{n(\mathbf{r})}\Delta n(\mathbf{r}), \tag{3.19}$$

$$\left[-\gamma\frac{\hbar^2}{2m}\nabla^2 + V_{eff} - \mu\right]\Delta\varphi(\mathbf{r}) = -[\Delta V_{eff}(\mathbf{r}) - \Delta\mu]\varphi(\mathbf{r}), \tag{3.20}$$

with

$$\Delta\mu = \int \varphi^*(\mathbf{r})\Delta V_{eff}(\mathbf{r})\varphi(\mathbf{r})d\mathbf{r}, \tag{3.21}$$

and the normalization condition

$$\int \varphi^*(\mathbf{r})\Delta\varphi(\mathbf{r})d\mathbf{r} = 0 \tag{3.22}$$

is implied.

The linear density response $\Delta n(\mathbf{r})$ is obtained by solving equations (3.18 $\div$ 3.20) with the conditions (3.21,3.22) self-consistently starting with the external perturbing $\Delta V_{ext}(\mathbf{r})$. The equation determining the change of the wave function (3.20) is similar to the so-called modified Sternheimer equation [51]. However, one needs to solve only one such equation to obtain the density response no matter how many electrons are present in the system. In the original scheme instead one equation for each occupied level needs to be solved. From the computational point of view, this reduction is very desirable especially for application to large systems.

The above procedure has been outlined for the case of static response-function. However, the calculation of RPA correlation energy in ACFD theory, as shown in Chapter 2,

or of van der Waals coefficients presented in the next section requires the determination of the response functions at finite imaginary frequencies. Fortunately, calculation of density responses at finite imaginary frequency can be done much in the same way with the only minor change that μ in equation (3.20) is replaced by $\mu + iu$ as shown in details by Mahan in the Ref. [52] or in a different derivation presented in Appendix A.

3.4 Polarizability and van der Waals coefficient in TFvW approximation

It is well know that when two atoms or molecules are far from each other so that the overlap of their electronic densities is essentially zero, they interact with each other via the so-called van der Waals force. In the non relativistic theory, interaction energy due to van der Waals force has a well known expression which is inversely proportional to the sixth power of the distance between the fragments

$$E(R) = -\frac{C_6}{R^6}, \tag{3.23}$$

where C_6 is called the van der Waals coefficient.

Calculation of van der Waals energy, i.e. of the asymptotic long-range interaction, is the most natural check for the validity of the approximate linear response functions by TFvW theory in capturing the non-local long-range interaction. This is done by calculating the van der Waals coefficients using the approximate scheme as described below. In fact, this kind of calculation must be performed in order to see if this approximate treatment of response functions is feasible for developing a density-based method that includes properly long-range correlations at any distances. van der Waals coefficient can be calculated via linear polarizabilities, $\alpha_{a,b}(iu)$, through the relation

$$C_{6,ab} = \frac{3}{\pi} \int du \alpha_a(iu) \alpha_b(iu). \tag{3.24}$$

In response to an external electric field, the system develops an induced moment which can be expressed in term of the field and polarizabilities. For example, a spherically

symmetric atom would develop a dipole moment p whose value is given by

$$p = \alpha\mathcal{E} + \frac{\gamma}{3!}\mathcal{E}^3 + ..., \tag{3.25}$$

where $\mathcal{E}$ is the strength of the field and α and γ are linear and nonlinear polarizabilities, respectively. For systems with high symmetry like spherical atoms, these quantities are scalars, but they can be tensors for lower symmetric systems.

In the expression of C_6 given above, $\alpha_{a,b}(iu)$ are linear polarizabilities depending on imaginary frequency iu of the fragments a and b. These quantities are not exactly the same as the static ones defined by (3.25), but the way they are calculated are essentially the same. By definition, linear polarizability can be computed from the density response $\Delta n(\mathbf{r}; iu)$ of the system under a constant external electric field $\mathcal{E}$ through the following expression

$$\alpha(iu) = \int \frac{z\Delta n(\mathbf{r}; iu)}{\mathcal{E}} d\mathbf{r}. \tag{3.26}$$

The linear response density $\Delta n(\mathbf{r}; iu)$ is obtained by solving self-consistently the set of equations from Eq. (3.18) to Eq. (3.20), replacing μ by $\mu + iu$, starting with the external perturbation $\Delta V_{ext}(\mathbf{r}) = e\mathcal{E}z$. Then the polarizability is easily calculated using expression (3.26).

In summary, van der Waals coefficient is obtained by the following steps.

i) Compute unperturbed ground state electronic density $n(\mathbf{r})$ via a standard Kohn-Sham self-consistent procedure within LDA or GGA.

ii) The effective potential $V_{eff}(\mathbf{r})$ is computed from $n(\mathbf{r})$ via Eq. (3.17) or the method described in the following section.

iii) For any given frequency iu, the density response $\Delta n(\mathbf{r}; iu)$ is calculated by solving the modified Sternheimer equation (3.18 $\div$ 3.22).

iv) Compute the polarizability $\alpha(iu)$ from $\Delta n(\mathbf{r}; iu)$ (Eq. 3.26).

v) Repeat steps *iii,* and *iv,* for each frequency iu.

vi) Compute C_6 from $\alpha(iu)$ (Eq. 3.24).

van der Waals coefficients between closed-shell ions have been computed in the framework of DFT by many authors over the years, starting by G.D. Mahan [52]. In these works the modified Sternheimer equations are solved for many occupied Kohn-Sham orbitals. The spherical symmetry of the considered systems is exploited in order to implement all-electron calculation in DFT framework within LDA. van der Waals coefficients as well as static polarizabilities obtained by Mahan and others are in good agreement with values from experiment or calculated by other methods. The calculation procedure, however, is demanding for larger and more complex systems. Our procedure, though being an approximation, is simpler because only one wave function needs to be computed instead of all electronic wave functions as in the method by Mahan. This advantage gives a chance to extend the calculation to complex systems, e.g. molecules or surfaces. We will compare with results in Ref. [52] in order to check the validity of the Thomas-Fermi and von Weizsäcker approximation for van der Waals coefficients.

3.5 Iterative procedure for construction of effective potential

As mentioned before for closed-shell spherical systems, direct determination of the effective potential, $V_{eff}(\mathbf{r})$, defined in Eq. (3.17) is not problematic since the numerical implementation is made simple by exploiting the spherical symmetry of the systems. The Kohn-Sham equations for determining the ground state charge density as well as the modified Sternheimer ones for calculating density response is solved on a radial grid with highly accurate Numerov's integration scheme. This leads to very accurate charge density, hence $\varphi(\mathbf{r})$, in the asymptotic regions. The effective potential therefore can be obtained from finite difference of expression (3.17), plus few iteration steps to add the corrections of order of square of grid spacing.

Unlike the case of closed-shell spherical ions, the effective potential can not always be obtained directly from its definition in the region where $\varphi(\mathbf{r})$ is vanishing. In the

plane-wave pseudopotential method for describing low symmetry systems, the charge density is calculated accurately up to a given cutoff of Fourier components. This gives insufficient numerical accuracy of the charge density, typically in the tail region of atoms and molecules where the density decays exponentially to zero. Unless very high kinetic-energy cutoff is used, the accuracy of $\varphi(\mathbf{r})$ obtained by simply taking the square root of the charge density as in definition (3.10) in the asymptotic region is not good enough which leads to noisy and unstable values for V_{eff} if evaluated directly from Eq. (3.17). In these region however the value of V_{eff} is not very relevant, exactly because the charge density is vanishing. The problem can be overcome by constructing the effective potential in an iterative process where at each iteration the corrective potential is smoothen so that at the end a smooth potential that admits $\varphi(\mathbf{r})$ as its ground state wave function is found. This iterative minimization process is similar to iterative construction of the optimized effective potential in Ref. [55] and can be described as follows.

Given an approximate $V_{eff}(\mathbf{r})$, a quantity $S(\mathbf{r})$, called residual, is defined by

$$\langle\varphi| - \frac{\hbar^2}{2m}\nabla^2 + V_{eff}(\mathbf{r})|\varphi\rangle = S(\mathbf{r}). \tag{3.27}$$

$S(\mathbf{r})$ vanishes at all points, $\mathbf{r}$, if $V_{eff}(\mathbf{r})$ is the desired potential that gives the ground state electronic density from equation (3.16). This effective potential can be found by an iterative procedure starting with a trial potential $V^0_{eff}(\mathbf{r})$. Let us denote $V^i_{eff}(\mathbf{r})$ and $S^i(\mathbf{r})$ the potential and the corresponding smooth correction at the step i of the iterative process. Since the potential is still not converged to the desired potential at this iteration, the smooth corrective potential $S^i(\mathbf{r})$ is still not identically vanishing to zero. The ground state density, $n^i(\mathbf{r})$, corresponding to the potential $V^i_{eff}(\mathbf{r})$ is found by solving equation (3.16). A new trial effective potential $V^{i+1}_{eff}(\mathbf{r})$ is then constructed from the old one by the relation

$$V^{i+1}_{eff}(\mathbf{r}) = V^i_{eff}(\mathbf{r}) + \alpha S^i(\mathbf{r}) + \beta. \tag{3.28}$$

With this expression, the new residual $S^{i+1}(\mathbf{r})$ is easily computed

$$S^{i+1}(\mathbf{r}) = S^i(\mathbf{r})[1 + \alpha n(\mathbf{r})] + \beta n(\mathbf{r}). \tag{3.29}$$

and the values of α and β are then obtained by minimizing the $\mathcal{L}_2 - norm$ of the new residual defined by

$$||S^{i+1}(\mathbf{r})|| = \int S^{i+1}(\mathbf{r})^2 d\mathbf{r}. \tag{3.30}$$

The procedure is repeated until the preset condition is fulfilled. In our calculation, it happens when the total absolute deviation of the charge density from the desired value

$$\delta n = \int |n(\mathbf{r}) - n^i(\mathbf{r})| d\mathbf{r} \tag{3.31}$$

is less than some given values (of the order of 10^{-2}).

This iterative procedure works well when only valence electrons are is taken into account. We have also calculated $V_{eff}(\mathbf{r})$ starting with densities having a core correction included. In these cases, the convergence rate of the iterative process becomes very slow even when a very large cut-off energy is used. Therefore, calculating an accurate effective potential in the presence of core density is presently impracticable. Although the role of core electrons is not negligible, we will show in the next chapter that core electrons have a very small effect on the value of van der Waals coefficients. For these reasons, core-electron charge-density will not be included when calculating the response functions in TFvW approximation for molecular systems.

Chapter 4

Applications to atomic and molecular systems

4.1 van der Waals coefficient of atoms and molecules

In order to calculate asymptotic long-range van der Waals interaction energies, we have implemented the scheme presented in Chapter 3 in the `atomic` code for suitable for the calculation of spherical atoms and in the `PWscf` plane-wave pseudopotential code for dealing with generic molecules. Both of them are part of the QUANTUM-ESPRESSO distribution [65] and our implementations are now distributed in the package. These implementations allow us to compute van der Waals coefficients by both the full (as already done for the case of closed-shell atoms and ions by Mahan [52]) and approximate (in the TFvW theory) treatments of the response function. The quality of TFvW approximation for linear response functions in capturing the long-range interactions will be observed by comparing the results of two calculations.

4.1.1 van der Waals coefficients of spherical atoms

Numerical results for closed-shell ions show a good agreement with those obtained by Mahan with an accurate but more expensive calculation for a wide range of atomic number

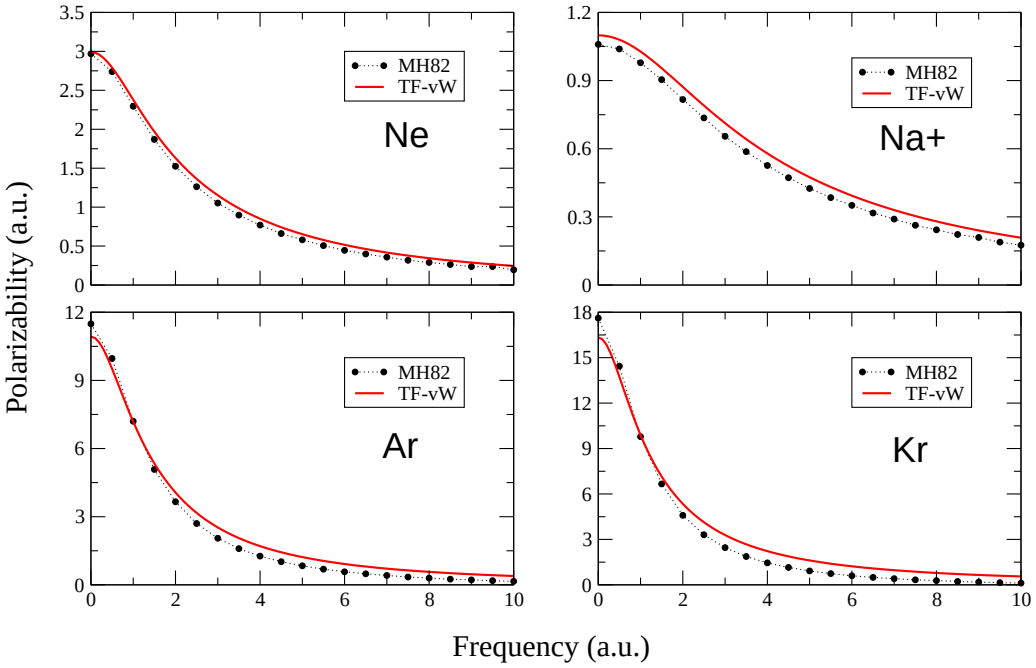

Figure 4.1: Dynamic polarizabilities of some spherical atoms calculated within the TFvW approach compared with the corresponding quantities computed by Mahan in Ref. [52].

and frequency. This can be seen in Fig. 4.1 where frequency-dependent polarizabilities of some closed-shell ions obtained by the two methods are compared. In Table 4.1 the results of vdW coefficients for a number of pairs of rare gases calculated using both full and approximate schemes are given. We also compare our results to those of Mahan's full calculation [52] and the results by Hult and co-workers in Ref. [67] where frequency-dependent polarizabilities of atoms and molecules were calculated by solving an electrodynamic equation with a crude treatment of dielectric functions by applying locally the expression for the dielectric function of the non-interacting homogeneous electron gas. Our results are all in the range and at least as accurate as those reported in Ref. [67] when compared to the reference ones. Note that there is a small discrepancy between our full calculation and those by Mahan. This is because we have been able to calculate atomic polarizabilities at high frequencies to numerically ensure the convergence of the integral for vdW cofficients from Eq. (3.24), while they were obtained by an extrapolation scheme in the calculations by Mahan.

Dimer	Present		Mahan	Unified	Reference
	TFvW	Full			
He	2.36	3.64	3.64	2.58	2.92
Ne	14.2	14.5	13.96	15.0	13.8
Ar	122	138	132.2	143	134
Kr	244	275	261.4	291	266
Xe	572	602	—	663	597

Table 4.1: C_6 values for dimers (Rydberg atomic units). Present: our results using both full and TFvW approaches. Mahan: calculations in the full approach by Mahan shown in Ref. [52]. Unified: calculations from Ref. [67] from solutions of an electrodynamic equation with a crude approximate dielectric function. Reference: Numbers quotes in Ref. [67].

In Fig. 4.2 our calculated C_6 values both for homonuclear and mixed pairs of 14 spherical ions are plotted against those reported in Ref. [52]. The good agreement between the results obtained by the two methods are indicated by the narrow spread of the points around the diagonal. Quantitatively, the difference never exceeds 25% and in most cases is less than 10% and improved for heavier atoms.

There are several factors that affect the values of the C_6 coefficients calculated above. First of all, the values of C_6 somehow depends on the quality of the charge density used as input for the calculation. For instance, using different xc-functionals in DFT calculation, i.e. slightly different but still accurate densities, leads to a slight change in the result of C_6 coefficients. Second, varying the values of γ which determines the von Weizsäcker gradient correction contribution in the TFvW approximate kinetic functional between 1 and 1/3 also changes the values of C_6. Calculations performed for all noble gas show however that final results are not sensitive to the parameter γ.

Finally, it is important to remind that our calculations using TFvW response functions

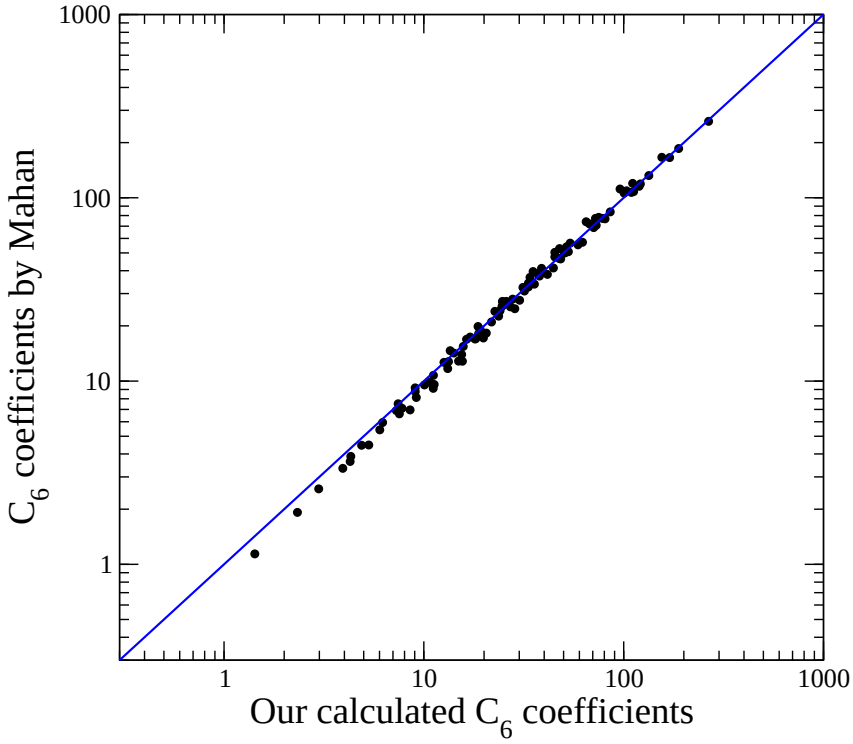

Figure 4.2: C_6 values of all possible pairs of 14 ions calculated by our method plotted (in logarithmic scale) against the corresponding values shown in Ref. [52]

are calculated around an accurate charge density. For this purpose, we need to introduce an effective potential admitting the square root of the charge density as its ground state wave function as already discussed in Chapter 3. One may wonder if this is indeed necessary since it seems natural to calculate the charge density also in TFvW approximation and then use it as input for the calculation of C_6 coefficient. Moreover, doing calculation in this way makes the construction of the effective potential needed in our calculation unnecessary because it is determined in the self-consistent solution of Eq. (3.16). We have tried this option for the case of noble gas atoms and the results is disastrous. For example, C_6 coefficient of He changes from 2.1 a.u. when computed with LDA-DFT charge density to 15.07, 36.38 and 227.15 (a.u.) when calculated with charge densities obtained from solution of the Hartree equation and self-consistent TF-vW approximation with $\gamma = 0.2$ and 1.0, respectively. This indicates the importance of calculating the response functions

with accurate charge densites. This is not totally unexpected since it is well-know that also the TFvW kinetic energy itself – the quantity on which the approximate response function is based – can give accurate estimates when applied to accurate charge density but behaves poorly if treated self-consistently. This shows that our approach, though still not being a self-consistent procedure (as commonly done in the EXX/RPA+ scheme or MBPT excited state calculations), is the correct way to calculate vdW coefficient using TF-vW approximation.

4.1.2 Effects of core electrons on polarizability and van der Waals coefficient

For systems not possessing spherical symmetry, the calculation of polarizability becomes much more complicated and more general computational methods which are available in modern electronic structure calculations, e.g. the plane-wave pseudopotential approach must be used. Most modern electronic structure calculations use pseudopotential approximation where only valence electrons are taken into account. This approximation allows to avoid the computational difficulties in dealing with localized core electrons but its validity fro the calculation of C_6 coefficients in the TFvW approach is unclear. Therefore, before considering more complicated systems, it is worthwhile to examine the contributions of core electrons to polarizabilities and van der Waals coefficients in a few atomic cases in order to see whether pseudopotential are also a good approximation for calculating van der Waals coefficients in this scheme.

This purpose have been done by comparing results of several atomic calculations where TFvW C_6 coefficients were computed starting from different charge densities used as input, namely all-electrons density, valence only density and valence density with part of core charge added as done in the non-linear core correction (nlcc) approximation [44]. Calculations have been done for two atoms: Beryllium and Argon. The number of core and valence electrons are comparable in these two atoms, but the atomic numbers are quiet different. Since Beryllium atom has two core and two valence electrons with small

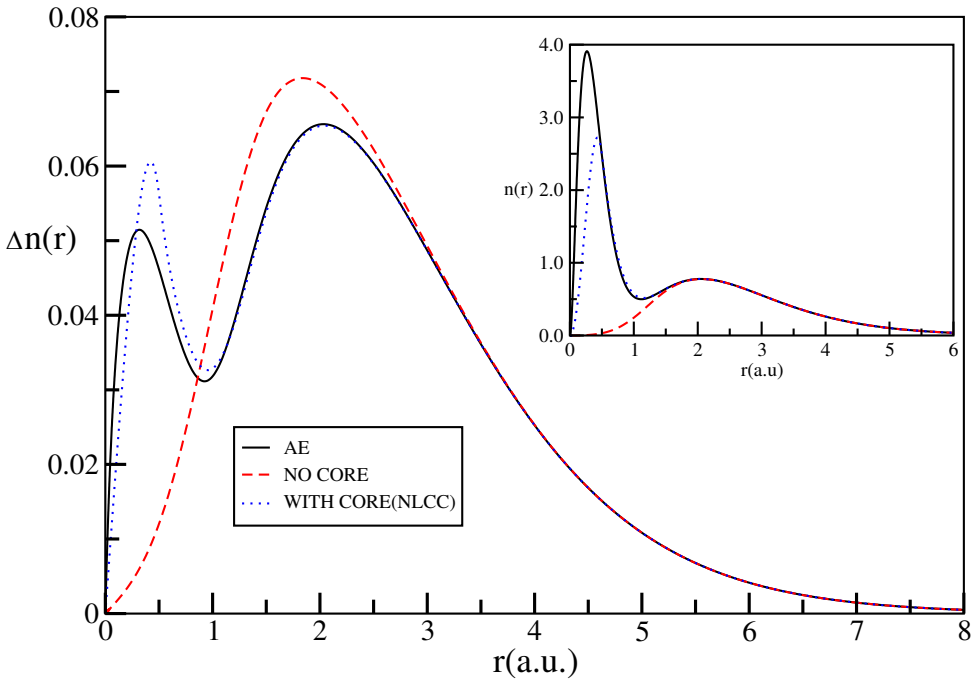

Figure 4.3: Radial part of the density responses of Be under a uniform electric field perturbation for all-electron (black solid curve), valence with nonlinear core correction (nlcc) (blue dotted curve), and valence only (red dashed curve) densities. The inset shows the corresponding unperturbed charge densities.

atomic number, the contribution of the core electrons to the total polarization of atom is perhaps significant. For the case of Argon atom, the number of core electrons is more than that of the valence ones. On the other hand, Argon has a large atomic number, hence, the core electrons are tightly-bound to the nucleus. The contribution of core electron in this case is expected to be small. It is interesting to note that the static polarizability of Be^{2+}, i.e. the polarizability of two core electrons alone is very small, less than 10^{-2} (in a.u.), and a similar result was found for the case of Argon. These observations lead to the expectation that the contribution of the core electrons to the total polarization of atoms is not considerable and it could be neglected in the calculations within plane-wave pseudopotential method.

Fig. 4.3 shows the radial part of the density responses of Beryllium atom under an uniform electric field calculated from three input electronic densities, namely all-electron

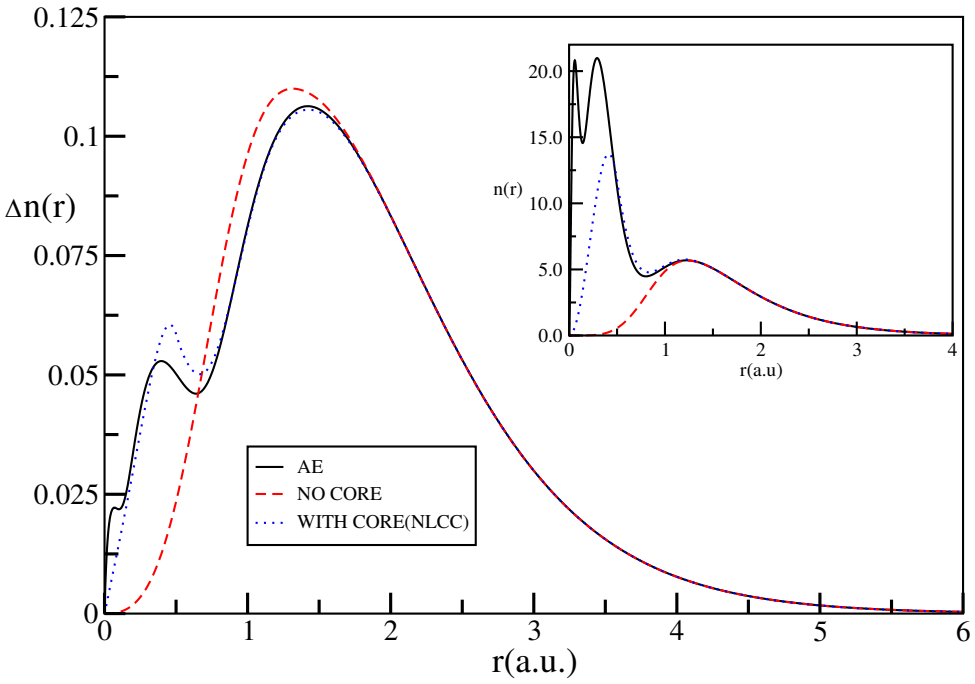

Figure 4.4: The same as in Fig. 4.3 but for Argon atom.

density, valence electron density including core charge in the nonlinear core correction approximation, and valence only density. Core electrons have two opposite effects on polarization of Beryllium atom. On the one hand, a large charge density in the core region leads to a large response density, i.e. makes polarizability increase. On the other hand, core charge prevents the penetration of valence electrons into the core region. In other words, it makes the valence electrons less polarizable, i.e. makes polarizability decrease. These effects do not cancel each other exactly, but still make the contribution of core electrons become less important. A similar behavior also appears in the case of Argon as shown in Fig. 4.4.

Table 4.2 gives static polarizabilities and van der Waals coefficients of Beryllium and Argon with the three kinds of charge densities. The results show that even for Beryllium, the contribution of core charge, expected to be significant, is just a few percent of the total van der Waals coefficient. A similar result is also present in the case of Argon. This is consistent with the observation about the role of core charge from static polarizability of ions composed of core electron only mentioned above. The results of Be and Ar lead us to

Atoms	$\alpha(0)$			C_6		
	ae	nlcc	valence	ae	nlcc	valence
Be	33.07	33.05	33.54	194.10	194.14	190.58
Ar	10.93	10.92	10.96	66.80	66.85	63.80

Table 4.2: Static polarizabilities $\alpha(0)$ and van der Waals coefficients C_6 (in Rydberg atomic units) for Be and Ar. The notations ae, nlcc and valence indicate the results obtained with all-electron, valence with nlcc and valence only densities.

the conclusion that van der Waals coefficients, in a good approximation, can be obtained in the Thomas-Fermi and von Weizsäcker method even when only valence electron density in a pseudopotential approximation is considered. This is a very useful property when extending the calculation to general system with the use of plane-wave basis set which would require enormous computational efforts when dealing with localized core electrons.

4.1.3 van der Waals coefficients of a few molecular systems

To exemplify the general scheme, we have calculated dynamic polarizabilities and vdW coefficients for a number of molecules. To show the efficiency of TFvW approximation, let us give here a more detailed investigation for the case of methane and benzene, two molecules with different nature of chemical bonds and geometric structures.

The KS equations for each isolated molecule were solved using periodic boundary condition in a simple cubic simulation cell with side length of 12 and 10 Å and kinetic-energy cutoffs of 80 and 60 Ry, respectively. Simple LDA exchange-correlation functional with norm-conserving pseudopotentials were used to obtain the GS charge density of the isolated molecules.

Fig. 4.5 shows the imaginary-frequency dynamic polarizabilities of methane and benzene molecules calculated in our scheme, compared with the result of the full calculation which has also been implemented in the `PWscf` plane-wave pseudopotential code. For

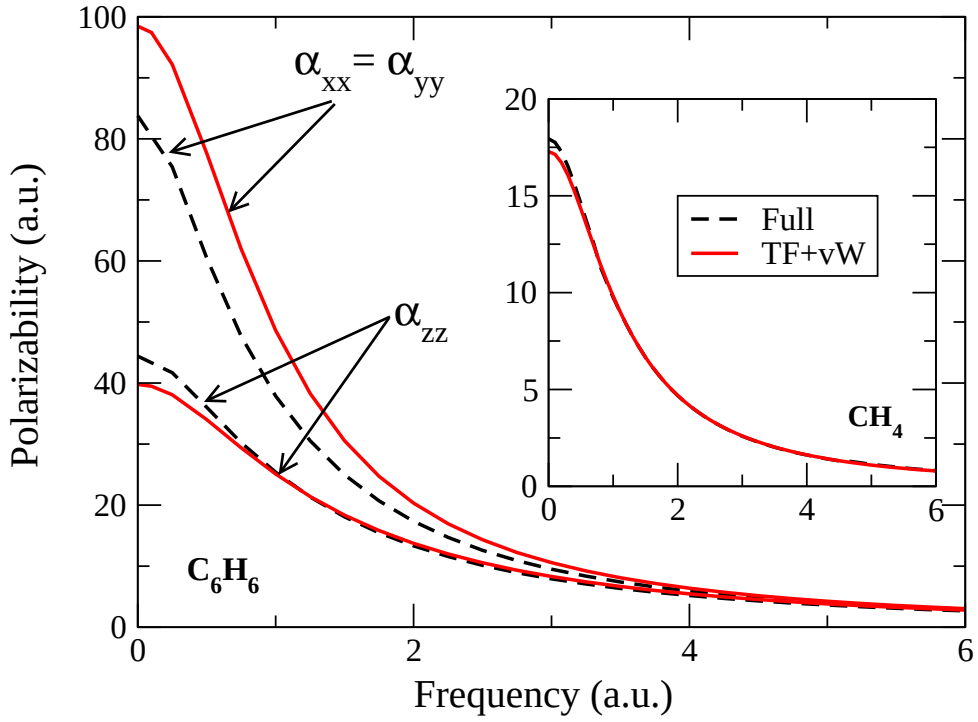

Figure 4.5: Imaginary-frequency dependent polarizabilities of methane (the inset) and benzene molecules calculated by TFvW method (solid red curves) compared to results of full calculation (dashed black curves).

methane molecule, the result of our simplified calculation compares excellently with the one of the more accurate method. Although this is not the case for benzene molecule, nevertheless the difference between the two calculations is still not very large.

Dimer	TF-vW	Full	Reference
CO_2	372	322	317
CH_4	264	271	259
C_6H_6	4956	3593	3446

Table 4.3: van der Waals C_6 coefficients (in the Rydberg atomic units) of CO_2, CH_4, and C_6H_6 molecules computed by full and simplified calculation compared with reference values obtained from the dipole oscillator strength distributions as quoted in Ref. [68]

Table 4.3 presents van der Waals C_6 coefficients of CO_2, CH_4, and C_6H_6 computed by full and simplified calculation in comparison with the reference values taken from the data quoted in the Ref. [68]. Very good agreement of the data is found for CO_2, CH_4 with strong covalent bonds, while the result from the simplified calculation for benzene is less impressive than those of other molecules. It is worth mentioning that the computational time required by the simplified calculation has been at least one order of magnitude lower than that of the full calculation and it is expected to become increasingly more convenient for larger systems.

4.2 RPA and RPA+ correlation energy of rare gas atoms

Let us now apply the scheme presented above to the calculation of RPA correlation energies for a number of spherical atoms. We exploit the symmetry of these systems to solve the Kohn-Sham and Sternheimer equations numerically on a logarithmic grid with the highly accurate Numerov's method. In spherically symmetric systems, ground state orbitals of Kohn-Sham system are classified by the principal quantum number n and the angular momentum numbers l, m and can be solved within a given LDA or GGA functional on a radial grid. The KS response function is block-diagonal and $(2l + 1)$-fold degenerate with respect to angular momentum number l and m, respectively. Thus diagonalization of χ_0 can be done independently for each block in the following steps:

i) Choose a potential to be considered as a perturbation and calculate the corresponding linear density response by solving the modified Sternheimer equation [51]. Note that this is the response of the non-interacting Kohn-Sham system, thus no self-consistent cycle needs to be performed in solving Sternheimer equation.

ii) Orthonormalize, with overlap matrix v_c, this density response to any previously computed one; the perturbation potential is transformed accordingly

since χ_0 is a linear operator; calculate the corresponding Hartree potential which will be used as the new trial perturbation.

iii) Build the matrix representation of the eigenvalue problem related to χ_0 in Eq. (2.18) by using the basis set composed of density responses, and then diagonalize it to get eigenvalues $\{a_\alpha\}$.

This three-step process is repeated until convergence in the sum over eigenvalues in Eq. (2.26) is reached. The same calculation procedure is then repeated at different values of iu (for integrating over imaginary frequency) and angular momentum. An efficient integration over imaginary frequency in Eq. (2.26) is obtained by dividing the frequency axis, from zero to a maximum values u_{max}, into many intervals and evaluating the integrated quantity in each interval by Gauss-Legendre method. While increasing the maximum value of the angular momenta, typically to $l_{max} = 20$ to get the the convergence within

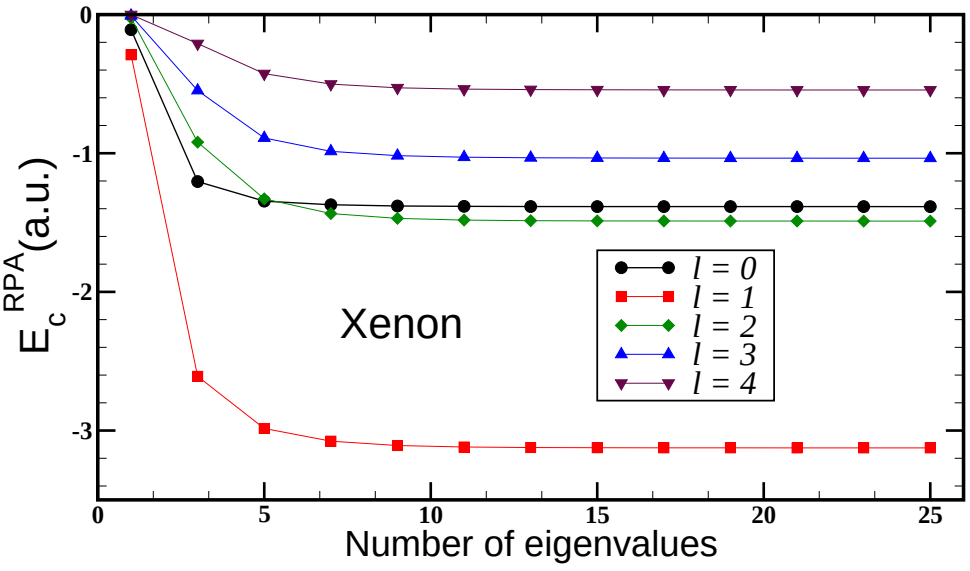

Figure 4.6: The dependence of RPA correlation energy on the number of eigenvalues for Xenon atom. The curves are for significant contributions to the total correlation energy from some of the lowest angular momentum numbers (higher l are not plotted.) Calculation up to 25 eigenvalues is enough to ensure a convergence within $1mRy$, which is also used as the threshold for convergence with respect to angular number l.

$1mRy$ of the correlation energy with respect to the summation over angular momenta, does not pose any problem, some difficulties do arise when increasing the maximum imaginary frequency, u_{max}, to get the same accuracy. Convergence within $1mRy$ with respect to the frequency integration of the correlation energy can only be achieved by integrating up to frequencies high enough that the absolute value of the integrand is as small as 10^{-8} Rydberg. This is very critical, especially for heavy atoms, since frequencies as high as 10^6 Ry must be considered and special care must be taken in order to reach this accuracy.

The difficulty arising at high frequencies stems from solving the modified Sternheimer equation numerically on a radial grid which is a boundary value problem whose asymptotic behaviors of the solution at the origin and infinity are known. Technically, the boundary value problem is usually turned into an initial value problem by assuming arbitrary values of the solution at the boundaries. The solution is then obtained by first integrating outward and inward to the classical turning point. The correct values of solution at two boundary points assumed arbitrary values before will be fixed using matching and smoothness conditions of the solution at the turning point. However, inward integration is performed for exponentially increasing function thus makes numerical values of the solution are easily become too large. One usually makes use of the linearity property of the second order differential equation (the modified Sternheimer equation) to do a trick by rescaling these values whenever they are larger than a given threshold. For the same system, the larger the imaginary frequency, the faster the solution increases, i.e. the larger is the number of rescaling required. A large number of rescaling will reduce numerical accuracy of the solution below the required level making iterative diagonalization procedure unstable. We have overcome this problem by replacing the inward and outward integration step by setting up a tridiagonal linear system whose solution can be easily obtained. Although, asymptotic behaviors of the solution of the Sternheimer equation near the origin and infinity are generally difficult to determine, they can be roughly approximated, e.g. assuming the same forms of the corresponding Schrödinger equation. The errors caused by this crude approximation can be reduced to an arbitrary small value by changing the values of the radial grid boundaries, namely reducing the value of the

boundary point near the origin and and increasing the value of the point considered to be at infinity.

Let us investigate the convergence of the RPA E_c with respect to the number of eigenvalues of the generalized eigenvalue problem (2.18) included in the summation in Eq. (2.26). Fig. 4.6 shows the dependence of RPA correlation energy – separated in different angular momentum contributions – on the number of eigenvalues for Xenon atom, the heaviest atom considered in this work. It is clearly seen that the correlation energies converge quite rapidly; including up to 25 eigenvalues is enough for a total correlation energy convergence within $1mRy$. These calculations therefore confirm explicitly, for the case of spherical atoms, our expectation that RPA correlation energy can be obtained

Table 4.4: Full RPA and RPA+ correlation energy (in Rydberg atomic units) of spherical atoms compared to the reference and exact values. The reference data were calculated from EXX-only (i.e. exact-exchange and no correlation) Kohn-Sham orbitals in a different implementation [14].

Atom	$^{\dagger}E_c^{\mathrm{expt}}$	E_c^{LDA}	E_c^{RPA}			$E_c^{\mathrm{RPA+}}$		
			ρ^{LDA}	ρ^{EXX}	Ref.	ρ^{LDA}	ρ^{EXX}	Ref.
He	-0.084†	-0.229	-0.168	-0.167	-0.166	-0.096	-0.094	0.094
Be	-0.190†	-0.447	-0.373	-0.367	-0.358	-0.230	-0.224	0.216
Ne	-0.786†	-1.474	-1.216	-1.195	-1.194	-0.821	-0.800	0.800
Ar	-1.463†	-2.842	-2.221	-2.206	-2.202	-1.503	-1.487	1.482
Kr	-4.15‡	-6.533	-5.226	-5.192	n/a	-3.736	-3.702	n/a
Xe	-6.86‡	-10.358	-8.312	-8.278	n/a	-6.049	-6.016	n/a

†Experimental values are those quoted in Ref. [37]. However, they are not available for Kr and Xe, and the corresponding numbers shown in the second column for these two atoms are correlation energies in the Hartree-Fock sense which are practically equal to correlation energies in DFT sense. Data were taken from A. Ma *et al.*, Phys. Rev. E **71**, 066704 (2005).

from only a relatively small number of eigenvalues of the problem (2.18).

Table 4.4 shows the full RPA and RPA+ correlation energies calculated in our implementation by using electronic densities from EXX-only[53] and standard LDA functionals. Experimental values and the data calculated from EXX-only charge densities with a different implementation[14] chosen as reference are also shown for comparison. All calculated values in Table 4.4 are accurate within a few mRy. The results slightly depend on the different xc-functionals used in the self-consistent calculation, i.e. on the different electronic densities used as input. Focusing on the results obtained starting from EXX-only charge densities, our calculated values for the full RPA correlation energy (the fifth column in the table) agree well with the reference data (sixth column) within the error bar (with the exception of Be case). The small residual differences between the values obtained in the two implementations may be attributed to a slight difference in the electronic densities used as input.

Not surprisingly, the RPA correlation energies alone indeed largely overestimate the exact values and when combined with local-density corrections to form the RPA+ approximation they become much closer to the exact values. Our calculations thus support the validity of RPA+ scheme.

4.3 Approximate RPA and RPA+ correlation energy of atoms

As a first step in an attempt to make the RPA+ scheme less computationally involved, we now explore the possibility to approximate the independent particle response functions by using Thomas-Fermi-von Weizsäcker (TFvW) kinetic energy functional. This approximation has the computationally desirable feature that it only involves a single auxiliary wave-function regardless of the number of electrons. As we have shown in the previous Sections, TFvW approximation can capture reasonably well asymptotic long

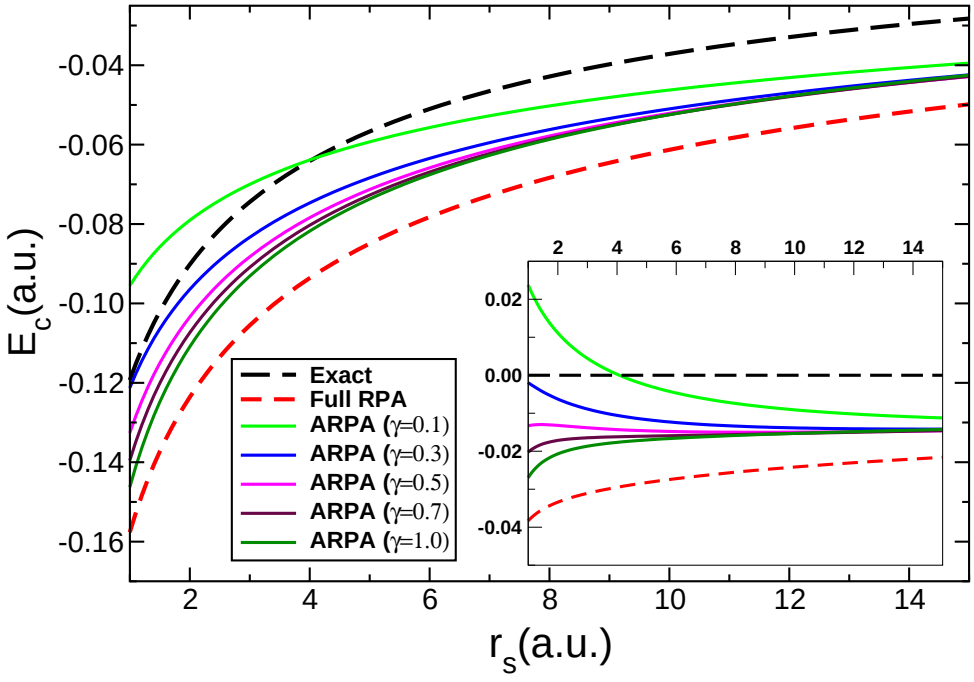

Figure 4.7: Full and approximate RPA correlation energies of uniform electron gas plotted as function of r_s. The inset shows data with exact correlation energy subtracted. For γ between 0.3 and 0.5, the difference of exact and TFvW approximate correlation energy is almost constant in a wide range of density.

range interactions via van der Waals coefficients. It is a purpose of the present section to demonstrate that TFvW approximation can be used also to calculate approximate, yet reasonably accurate, correlation energies with much less computational effort with respect to the full RPA calculation.

For the case of free electron gas, TFvW approximation to the kinetic energy alone at a given value of parameter γ which determines the contribution of von Weizsäcker gradient correction to the kinetic energy gives the following expression for the response function at imaginary frequency, iu, wave-vector, q:

$$\tilde{\chi}_0(q,u;\gamma) = -\frac{3n}{2\varepsilon_F}\left[1+\frac{3}{4}\frac{\gamma^2\tilde{q}^4+4\tilde{u}^2}{\gamma\tilde{q}^2}\right]^{-1}, \tag{4.1}$$

where $\tilde{q}=q/k_F$ and $\tilde{u}=u/(2\varepsilon_F)$ with ε_F, k_F and n being Fermi energy and Fermi wave-vector and electronic density, respectively. It can be noted that this response function

is exact in two limits: the limit of long-wavelength when $\gamma = 1/9$, and the limit of short-wavelength with $\gamma = 1$. This explains why in practical applications of the TFvW approximation the value of γ in the range between these two limiting values has often been chosen. Although solving Dyson-like equation is very demanding in general, it is extremely simplified for uniform electron gas where linear response functions are diagonal in reciprocal space due to translational invariance. The full RPA correlation energy and the approximate one in TFvW approximation are easily computed for the jellium model from the exact Lindhard's function and the approximate $\tilde{\chi}_0(q, u; \gamma)$ above, respectively, and are plotted for several values of γ in Fig. 4.7.

It is clearly seen that for all values of γ between 0 and 1 and for a wide range of density, the approximate RPA (ARPA) correlation energies are closer to the exact value than those from full RPA. Moreover, for γ in the range between 0.3 and 0.5, the difference between the approximate and exact correlation energy is almost constant in the range of densities show in the figure. This suggests to use a kind of local-density correction to the correlation energy calculated from the approximate linear response function by using TFvW functional in the spirit of RPA+. In order to apply the Local Density correction to the approximate RPA correlation a parametrization of the ARPA correlation energy for the electron gas is needed. We have chosen to parametrize these data by Perdew-Zunger's formula for spin unpolarized electron gas [43] and namely by

$$\epsilon_c = \frac{\gamma}{\beta_1 \sqrt{r_s} + \beta_2 r_s} \tag{4.2}$$

with $\gamma = -0.1423, \beta_1 = 1.0529, \beta_2 = 0.3334$ for $r_s \geq 1$, i.e. in the high density limit, and

$$\epsilon_c = A \ln(r_s) + B + C r_s \ln(r_s) + D r_s \tag{4.3}$$

with $A = 0.0311, B = -0.048, C = 0.0020, D = -0.0116$ for $r_s \geq 1$, i.e. in the intermediate and low density limit. This parametrization will to be used later in the calculation of short-range correction in the RPA+ scheme.

For a general non homogeneous system, the TFvW functional can be used to calculate linear response functions in an approximate manner following much the same procedure

outlined earlier for the full RPA calculation. But here it is simplified by the fact that linear density response corresponding to a trial perturbation ΔV is obtained by solving a kind of modified Sternheimer equation involving only one auxiliary normalized wavefunction, φ, which is the square root of the density, Eqs. (3.18 $\div$ 3.20), instead of the multi-band procedure of DFPT.

Approximate RPA and RPA+ correlation energies calculated within the scheme outlined above are shown in Table 4.5 for several values of γ. Again all calculated values here are accurate to within a few mRy and convergence with respect to imaginary frequency was carefully checked. The general trend is that approximate RPA correlation energies stay in between the exact (experimental) and full RPA values. This is consistent with the behavior shown in Fig. 4.7 for the homogeneous electron gas. Although the approximate RPA E_c depends on the value of γ, the dependence is rather mild. When we include a local-density correction to the approximate RPA (ARPA) energies, we obtain the approximate RPA+ (ARPA+) energies, whose magnitude increases as γ decreases from 1 to 0. They also do not depend sensitively on the parameter γ and a good agreements with experimental results–as good as that obtained for the full RPA+ calculation—is found for a range of γ between 0.3 and 0.5. These results suggest a possible strategy to efficiently calculate accurate correlation energies in van der Waals systems where standard DFT with LDA or GGAs alone does not give satisfactory descriptions.

Table 4.5: Full (E_c^{RPA}) and approximate (E_c^{ARPA}) correlation energies in TFvW approximation at several values of γ for various spherical atoms calculated by using LDA KS orbitals. Correlation energies in RPA+ scheme, denoted $E_c^{\mathrm{RPA+}}$ and $E_c^{\mathrm{ARPA+}}$, are also presented. The results show that when γ is in the range between 0.3 and 0.5, the approximate scheme gives results as good as those obtained in the full calculations compared to experimental values (energies are in Rydberg atomic units.)

		Full RPA		ARPA: $\gamma = 0.7$		ARPA: $\gamma = 0.5$		ARPA: $\gamma = 0.4$		ARPA: $\gamma = 0.3$		ARPA: $\gamma = 0.1$	
Atom	$^{\ddagger}E_c^{\mathrm{expt}}$	E_c^{RPA}	$E_c^{\mathrm{RPA+}}$	E_c^{ARPA}	$E_c^{\mathrm{ARPA+}}$	E_c^{ARPA}	$E_c^{\mathrm{ARPA+}}$	E_c^{ARPA}	$E_c^{\mathrm{ARPA+}}$	E_c^{ARPA}	$E_c^{\mathrm{ARPA+}}$	E_c^{ARPA}	$E_c^{\mathrm{ARPA+}}$
He	**-0.0840**	-0.168	**-0.096**	-0.086	-0.046	-0.093	**-0.067**	-0.098	**-0.080**	-0.102	**-0.097**	-0.105	-0.146
Be	**-0.1900**	-0.373	**-0.230**	-0.202	-0.121	-0.215	**-0.161**	-0.222	**-0.187**	-0.228	**-0.218**	-0.221	-0.307
Ne	**-0.786**	-1.216	**-0.821**	-0.809	-0.573	-0.828	**-0.697**	-0.833	**-0.775**	-0.830	**-0.865**	-0.743	-1.121
Ar	**-1.463**	-2.221	**-1.503**	-1.706	-1.263	-1.717	**-1.492**	-1.709	**-1.630**	-1.683	**-1.790**	-1.455	-2.239
Kr	**-4.15**	-5.226	**-3.736**	-4.362	-3.385	-4.296	**-3.868**	-4.220	**-4.152**	-4.089	**-4.477**	-3.361	-5.353
Xe	**-6.86**	-8.312	**-6.049**	-7.268	-5.739	-7.088	**-6.463**	-6.921	**-6.884**	-6.741	**-7.445**	-5.338	-8.620

‡Experimental values are those quoted in Ref. [37]. However, they are not available for Kr and Xe, and the corresponding numbers shown in the second column for these two atoms are correlation energies in the Hartree-Fock sense which are practically equal to correlation energies in DFT sense. Data were taken from A. Ma *et al.*, Phys. Rev. E **71**, 066704 (2005).

Conclusion

In the present thesis a new computational strategy for the calculation of RPA correlation energy in the Adiabatic Connection Fluctuation-Dissipation formalism has been proposed. Technical details of the method as implemented in the plane-wave pseudopotential approach were discussed at some level. The implementation has been applied to study bulk silicon system and Beryllium dimer which demonstrate the efficiency of the method. We have also investigated the possibility to approximate the response functions needed to be diagonalized for calculating correlation energy in our method by using the Thomas-Fermi-von Weizsäcker approximation for the (non-interacting) kinetic energy functional. This approximate scheme is computationally much less involved, especially for large systems, and has been applied to several test cases with promising results.

LDA or GGA treatments of xc-energy in DFT calculation is known to fail for systems where long-range correlations play an important role, and an alternative promising approach where the correlation energy is treated in RPA approximation for the xc-kernel in the ACFD theory has been proposed and investigated recently. Existing plane-wave pseudopotential implementations for the calculation of RPA correlation energy in ACFD formalism [12, 13, 15] usually follow the same strategy, namely the calculation of the non-interacting Kohn-Sham response function by performing a cumbersome summation over occupied and empty states, and the calculation of the interacting response function at a given coupling constant by the solution of a Dyson-like equation relating it to the non-interacting one. Our implementation is based on the calculation of a rather small number of eigenvalues of the RPA dielectric function by an iterative diagonalization procedure where the well-established and very efficient techniques of Density Functional Perturba-

tion Theory can be used. Although the scaling of the needed computational effort in our implementation is not better than that of the existing ones (growing as the power fourth of the system size), this new implementation is more efficient since its scaling pre-factor is at least two order of magnitude smaller.

The validity of our implementation has been carefully checked by applying to several systems which have been studied in other implementations before. While the study of bulk silicon crystal helps to validate the implementation and to develope an extrapolation scheme useful for the treatment of larger systems, our study of Beryllium dimer, thanks to its better numerical accuracy as compared with previous studies [12], allows us to have a clearer picture of the performance of EXX/RPA+ scheme in describing weakly bound systems where this scheme is expected to perform well. Our calculation confirms the important improvements of EXX/RPA+ with respect to LDA or GGA due to a more accurate treatment of the xc-energy but also shows that its performance in the delicate case of Be dimer is less impressive than previously concluded. The possibility of a careful control of numerical accuracy will be useful for application of the method to other realistic systems.

Since the calculation of RPA correlation energy in ACFD formalism is very computationally demanding, it becomes impractical when the size of the system is large, even within a very efficient implementation. A possibile strategy to make this calculation less computationally demanding by using approximate Thomas-Fermi-von Weizsäcker response functions in the evaluation RPA correlation energy has been proposed and studied in this thesis. This approximation is very computationally desirable since application of the response function to a trial potential, which is performed routinely in our implementation of ACFD method can be obtained by solving only one DFPT-type equation instead of a multitude, as needed in the full treatment, no matter how many electrons are present in the system. The potential of this approximate scheme in capturing the long-range correlations has been shown by a good agreement, typically within 20%, of the van der Waals coefficients calculated with approximate and full response functions for a number of closed-shell atoms and molecules. Approximate RPA and RPA+ correlation energies,

i.e. energies calculated with the same procedure used for the full RPA correlation energy in ACFD formalism but using approximate response functions as ingredients, have been calculated for a number of rare-gas atoms and the results show the promise of the approximation. Although more systematic calculations of this approximate scheme needs to be performed for more realistic systems in order to assess its quality, we believe that this approximate scheme would be useful in the treatment of large systems to some degree of accuracy.

In conclusion our implementation of a new computational strategy for RPA correlation energy in ACFD theory is presented and the results obtained from a few case studies have shown the efficiency of the method. The implementation allows us to be able to perform accurate calculations on very weakly bound systems which is important for assessing the accuracy of RPA xc-kernel. Our implementation can be easily adapted to use approximate response functions in order to make it less computationally demanding at the price of making it more approximate. An approximation base on the Thomas-Fermi-von Weizsäcker scheme has been explicitly tested. From the results of some test cases, we believe that, although this approximation may not be able to give very accurate description of the correlation energy, it can capture long-range correlations to some degree of accuracy and thus can be useful for many applications where van der Waals interaction plays important role.

Appendix A

Response function at finite imaginary frequency

In this appendix, the derivation is given for the result quoted in Chapter 2 that density-response to a static perturbation calculated at finite imaginagy frequency, iu, of the Kohn-Sham response function can be obtained with the same procedure used for zero frequency just replacing the eigenvalue ϵ_i in the Sternheimer of DFPT equation by $\epsilon_i + iu$.

Let us start with the well-known expression for $\chi_0(\mathbf{r}, \mathbf{r}'; iu)$

$$\chi_0(\mathbf{r}, \mathbf{r}'; iu) = \sum_{i,j} \frac{f_i - f_j}{\epsilon_i - \epsilon_j + iu} \phi_i^*(\mathbf{r})\phi_j(\mathbf{r})\phi_j^*(\mathbf{r}')\phi_i(\mathbf{r}'), \tag{A.1}$$

where $\{\epsilon_i\}$ and $\{\phi_i(\mathbf{r})\}$ are the sets of eigenvalues and eigenfunctions of the Kohn-Sham Hamiltonian $-\frac{1}{2}\nabla^2 + V_{KS}(\mathbf{r})$, respectively, and f_i being the occupation of state $\phi_i(\mathbf{r})$.

By definition, density response $\Delta n(\mathbf{r}; iu)$ at finite imaginary frequency iu corresponding to a given perturbation potential $\Delta V(\mathbf{r})$ is

$$\Delta n(\mathbf{r}; iu) = \int d\mathbf{r}' \chi_0(\mathbf{r}, \mathbf{r}'; iu) \Delta V(\mathbf{r}') \tag{A.2}$$

Replacing χ_0 in Eq. (A.2) by its expression in Eq. (A.1) we get

$$\begin{aligned}\Delta n(\mathbf{r};iu) = & \sum_{i,j} f_i \frac{\phi_i^*(\mathbf{r})\phi_j(\mathbf{r})}{\epsilon_i - \epsilon_j + iu} \int d\mathbf{r}' \phi_j^*(\mathbf{r}')\Delta V(\mathbf{r}')\phi_i(\mathbf{r}') \\ + & \sum_{i,j} f_j \frac{\phi_i^*(\mathbf{r})\phi_j(\mathbf{r})}{\epsilon_j - \epsilon_i - iu} \int d\mathbf{r}' \phi_j^*(\mathbf{r}')\Delta V(\mathbf{r}')\phi_i(\mathbf{r}'). \end{aligned} \tag{A.3}$$

Interchanging the dummy indices i and j in the second term, one can show that the two terms are indeed complex conjugate. Therefore, one can write the expression for $\Delta n(\mathbf{r};iu)$ in a form which is more convenient for computational purpose.

$$\Delta n(\mathbf{r};iu) = 2Re\{\sum_i f_i \phi_i^*(\mathbf{r})\Delta\phi_i(\mathbf{r};iu)\}, \tag{A.4}$$

with

$$\Delta\phi_i(\mathbf{r};iu) = \sum_j \phi_j(\mathbf{r}) \int d\mathbf{r}' \frac{\phi_j(\mathbf{r}')\Delta V(\mathbf{r}')\phi_i(\mathbf{r}')}{\epsilon_i - \epsilon_j + iu} \tag{A.5}$$

Note that the occupation number f_i vanishes if the energy ϵ_i belongs to the unoccupied bands and $\Delta\phi_i(\mathbf{r};iu)$ needs to be computed for the occupied levels only.

Let us find an equation for this quantity by applying the Kohn-Sham Hamiltonian to it

$$\begin{aligned}[-\frac{1}{2}\nabla^2 + V_{KS}(\mathbf{r}) - \epsilon_i - iu]\Delta\phi_i(\mathbf{r};iu) &= \sum_j (\epsilon_j - \epsilon_i - iu)\phi_j(\mathbf{r}) \int d\mathbf{r}' \frac{\phi_j(\mathbf{r}')\Delta V(\mathbf{r}')\phi_i(\mathbf{r}')}{\epsilon_i - \epsilon_j + iu} \\ &= -\int d\mathbf{r}' \{\sum_j \phi_j(\mathbf{r})\phi_j(\mathbf{r}')\}\Delta V(\mathbf{r}')\phi_i(\mathbf{r}') \\ &= -\int d\mathbf{r}' \delta(\mathbf{r} - \mathbf{r}')\Delta V(\mathbf{r}')\phi_i(\mathbf{r}') \\ &= -\Delta V(\mathbf{r})\phi_i(\mathbf{r}). \end{aligned}$$

Hence we avoid the cumbersome summation over all unoccupied states in Eq. (A.1) or (A.5) by solving the following linear equation for each occupied state

$$[-\frac{1}{2}\nabla^2 + V_{KS}(\mathbf{r}) - \epsilon_i - iu]\Delta\phi_i(\mathbf{r};iu) = -\Delta V(\mathbf{r})\phi_i(\mathbf{r}). \tag{A.6}$$

This can be done efficiently by iterative techniques.

Appendix B

Note for calculation of spin-polarized systems

In this appendix, we show that the procedure presented in Chapter 2 for calculating E_c in the ACFD formalism for spin-unpolarized systems in RPA approximation is still applicable to the case of spin-polarized systems with appropriate definition of the response functions.

Let us start with a generalization of the relation between xc-energy and response function for the case of spin-polarized systems

$$E_c = -\frac{\hbar}{2\pi}\int_0^1 d\lambda \int d\mathbf{r}d\mathbf{r}' v_c(\mathbf{r},\mathbf{r}') \times \int_0^\infty du \sum_{\sigma,\sigma'}[\chi_\lambda^{\sigma\sigma'}(\mathbf{r},\mathbf{r}';iu) - \chi_0^{\sigma\sigma'}(\mathbf{r},\mathbf{r}';iu)], \quad \text{(B.1)}$$

with both non-interacting Kohn-Sham response function and the interacting one becoming a 2×2 matrix, though the non-interacting one is still diagonal in spin-space, i.e. $\chi_0^{ud} = \chi_0^{du} = 0$. The Dyson-like equation that relates the interacting to the non-interacting response function in this case reads

$$\chi_\lambda^{\sigma\sigma'} = \chi_0^{\sigma\sigma'} + \sum_{\nu,\nu'} \chi_0^{\sigma\nu}(v_c + f_{xc}^{\nu\nu'})\chi_\lambda^{\nu'\sigma'}, \quad \text{(B.2)}$$

where integration over spatial coordinates on the right-hand-side is implicitly implied and the Coulomb kernel v_c couples in the same way all spin components to each other. In

RPA, xc-kernel f_{xc} is set to zero, and the Dyson-like equation can be written in matrix form as

$$\begin{pmatrix} \chi_\lambda^{uu} & \chi_\lambda^{ud} \\ \chi_\lambda^{du} & \chi_\lambda^{dd} \end{pmatrix} = \begin{pmatrix} \chi_0^{uu} & 0 \\ 0 & \chi_0^{dd} \end{pmatrix} + \begin{pmatrix} \chi_0^{uu} & 0 \\ 0 & \chi_0^{dd} \end{pmatrix} \begin{pmatrix} v_c & v_c \\ v_c & v_c \end{pmatrix} \begin{pmatrix} \chi_\lambda^{uu} & \chi_\lambda^{ud} \\ \chi_\lambda^{du} & \chi_\lambda^{dd} \end{pmatrix}. \quad \text{(B.3)}$$

If we define

$$\chi_0 = \chi_0^{uu} + \chi_0^{dd}, \quad \text{(B.4)}$$

$$\chi_\lambda = \chi_\lambda^{uu} + \chi_\lambda^{ud} + \chi_\lambda^{du} + \chi_\lambda^{dd}, \quad \text{(B.5)}$$

then after some trivial algebra we get

$$\chi_\lambda = \chi_0 + \chi_0 v_c \chi_\lambda, \quad \text{(B.6)}$$

which is exactly the same formula as for spin-unpolarized systems.

With the note that $Tr(A+B) = Tr(A) + Tr(B)$ and the trace of a matrix is invariant under a similarity transformation, it is easy to see that E_c of spin-polarized systems can be calculated with the same procedure used for spin-unpolarized case discussed in Chapter 2. The only thing that needs to be changed here is that χ_0 is now the sum of the responses of spin-up and spin-down electron-densities to the same perturbing potential.

Bibliography

[1] P. Hohenberg and W. Kohn, Phys. Rev. **136**, B864 (1964).

[2] W. Kohn and L.J. Sham, Phys. Rev. **140**, A1133 (1965).

[3] O. Gunnarsson and B.I. Lundquist, Phys. Rev. B **13**, 4274 (1976).

[4] A. D. Becke, Phys. Rev. A **38**, 3098 (1988); J. P. Perdew, K. Burke and M. Ernzerhof, Phys. Rev. Lett. **77**, 3865 (1996).

[5] A. D. Becke, J. Chem. Phys. **98**, 1372 (1993).

[6] W. Kohn, Y. Meir, and D. E. Makarov Phys. Rev. Lett. **80**, 4153 (1998).

[7] D. C. Langreth, J. P. Perdew, Solid State Commun. **17**, 1425 (1975); D. C. Langreth, J. P. Perdew, Phys. Rev. B **15**, 2884 (1977).

[8] M. Dion *et al.*, Phys. Rev. Lett. **92**, 246401 (2004).

[9] T. Thonhauser *et al.*, Phys. Rev. B **76**, 125112 (2007)

[10] F. Furche, Phys. Rev. B **64**, 195120 (2001)

[11] F. Furche and T. Van Voorhis, J. Chem. Phys. **122**, 164106 (2005)

[12] M. Fuchs and X. Gonze, Phys. Rev. B **65**, 235109 (2002).

[13] A. Marini, P. García-González, J. J. Fernández, and A. Rubio, Phys. Rev. Lett. **96**, 136404 (2006); P. García-González, J. J. Fernández, A. Marini and A. Rubio, J. Phys. Chem. A. **111**, 12458 (2007)

[14] H. Jiang and E. Engel, J. Chem. Phys. **127**, 184108 (2007).

[15] J. Harl and G. Kresse, Phys. Rev. B **77**, 045136 (2008).

[16] M. Born and J. R. Oppenheimer, Ann. Physik **84**, 457 (1927).

[17] D. R. Hartree, Proc. Cambridge Phil. Soc. **111**, 426 (1928).

[18] E. A. Hylleraas, Z. Phys. **54**, 347 (1929); *ibid* **65**, 209 (1930).

[19] V. Fock, Z. Phys. **61**,126 (1930).

[20] L. H. Thomas, Proc. Cambridge Philos. Soc. **23**, 542 (1927).

[21] E. Fermi, Z. Phys. **48**, 73 (1928).

[22] P. A. M. Dirac, Proc. Cambridge Phil. Roy. Soc. **26**, 376 (1930).

[23] D. M. Ceperley and B. J. Alder, Phys. Rev. Lett. **45**, 566 (1980).

[24] See, e.g., W. H. Press, S. A. Teukolsky, W. T. Vetterling, and B. P. Plannery *"Numerical Recipes: The Art of Scientific Computing*, Vol. I, second edition, Cambridge University Press (1992).

[25] D. R. Hamann, M. Schluter and C. Chiang, Phys. Rev. Lett. **43**, 1494 (1979).

[26] D. Vanderbilt, Phys. Rev. B **41**, 7892 (1990).

[27] See, for example, X. Wu, M. C. Vargas, S. Nayak, V. Lotrich, and G. Scoles, J. Chem. Phys. **115**, 8748 (2001).

[28] S. Grimme, J. Comput. Chem. 25, 1463 (2004).

[29] X. Xu and W. A. Goddard III, Proc. Natl. Acad. Sci. U.S.A. **101**, 2673 (2004); J. T. Su, X. Xu, and W. A. Goddard III, J. Phys. Chem. A **108**,10518 (2004).

[30] S. Baroni, P. Giannozzi, and A. Testa, Phys. Rev. Lett. **58**, 1861 (1987); S. Baroni, A. Dal Corso, P. Giannozzi, and S. de Gironcoli, Rev. Mod. Phys. **73**, 515 (2001).

[31] H. B. Callen and T. A. Welton, Phys. Rev. **83**, 34 (1951).

[32] E. K. Gross and W. Kohn, Phys. Rev. Lett. **55**, 2850 (1985).

[33] A. Görling, Phys. Rev. Lett. **83**, 5459 (1999); F. D. Sala and A. Görling, J. Chem. Phys. **115**, 5718 (2001).

[34] M. Städele, J. A. Majewski, P. Vogl, and A. Görling, Phys. Rev. Lett. **79**, 2089 (1997); C. M. Horowitz, C. R. Proetto, and S. Rigamonti, Phys. Rev. Lett. **57**, 14974 (2006).

[35] G. Onida, L. Reining, and A. Rubio, Rev. Mod. Phys. **74**, 601 (2002).

[36] M. Petersilka, U. J. Gossmann, and E. K. U. Gross, Phys. Rev. Lett. **76**, 1212 (1996).

[37] S. Kurth and J. P. Perdew, Phys. Rev. B **59**, 10461 (1999).

[38] Z. Yan, J. P. Perdew, and S. Kurth, Phys. Rev. B **61**, 16430 (2001).

[39] J. F. Dobson, J. Wang, Phys. Rev. B, **62**, 10038 (2000); J. M. Pitarke, J. P. Perdew, Phys. Rev. B **67**, 045101 (2003); J. Jung, P. García-González, J. F. Dobson, and R. W. Godby, Phys. Rev. B **70**, 205107 (2004).

[40] K. S. Singwi, M. P. Tosi, R. H. Land, and A. Sjölander, Phys. Rev. **176**, 589 (1963).

[41] K. Rapcewicz and N. W. Ashcroft, Phys. Rev. B **44**, 4032 (1991).

[42] Y. Andersson, D.C. Langreth, and B. I. Lundqvist, Phys. Rev. Lett. **76**, 102 (1996).

[43] J. P. Perdew and A. Zunger, Phys. Rev. B **23**, 5048, (1981).

[44] S. G. Louie, S. Froyen, and M. L. Cohen, Phys. Rev. B, **26** (1982).

[45] C. F. von Weizäcker, Z. Phys. **96**, 431 (1935).

[46] See, e.g in the review by N. H. March, Adv. in Physics **6**, 1 (1957).

[47] P. L. Gombas, Phys. Lett. A **28A**, 585 (1969).

[48] H. M. Schey and J. L. Schwartz, Phys. Rev. **137**, A709 (1965).

[49] W. Jones and W. H. Young, J. Phys. C **4**, 1322 (1971).

[50] R. M. Dreizler and E. K. U. Gross, *Density Functional Theory*, Springer-Verlag, Berlin (1990).

[51] G. D. Mahan, Phys. Rev. A **22**, 1780 (1980).

[52] G. D. Mahan, J. Chem. Phys. **76**, 493 (1982).

[53] A. Goerling, and M. Levy, Phys. Rev. A **50**, 196 (1994); R.J. Magyar, A. Fleszar, and E.K.U. Gross, Phys. Rev. B **69**, 045111 (2004).

[54] G. D. Mahan and K. R. Subbaswamy, *Local Density Theory of Polarizability*, (Plenum, New York 1990), pp 46-48.

[55] S. Kümmel and J. P. Perdew, Phys. Rev. Lett. **90**, 043004 (2003).

[56] J. F. Dobson and J. Wang Phys. Rev. Lett. **82**, 2313 (1999).

[57] A. Baldereschi and E. Tosatti, Solid State Commun. **29**, 131 (1979); R. Car, E. Tosatti, S. Baroni, and S. Leelaprute, Phys. Rev. B **24**, 985 (1981); M. Hybertsen and S. G. Louie, *ibid.* **35**, 5585 (1987).

[58] H. Wilson, F. Gygi, and G. Galli, Phys. Rev. B **78**, 113303 (2008).

[59] D. Lu, F. Gygi and G. Galli, Phys. Rev. Lett. **100**, 147601 (2008).

[60] H. J. Monkhorst and J. D. Pack, Phys. Rev. B **13**, 5188 (1976); A. Baldereschi, Phys. Rev. B **7**, 5212 (1973); D. J. Chadi and M. L. Cohen, Phys. Rev. B **7**, 692 (1973).

[61] Y. Saad and M. Schulz, SIAM Journal on Scientific and Statistical Computing, **7**, 856, (1986).

[62] H. van der Vorst, SIAM J. Sci. Stat. Comput. **13**, 631 (1992).

[63] O. H. Nielsen and R. M. Martin, Phys. Rev. B **32** 3787 (1985).

[64] S. Baroni, A. Dal Corso, S. de Gironcoli, P. Giannozzi, C. Cavazzoni, G. Ballabio, S. Scandolo, G. Chiarotti, P. Focher, A. Pasquarello, K. Laasonen, A. Trave, R. Car, N. Marzari, A. Kokalj, http://www.pwscf.org/.

[65] QUANTUM-ESPRESSO is a community project for high-quality quantum-simulation software, based on density-functional theory, and coordinated by Paolo Giannozzi. See http://www.quantum-espresso.org and http://www.pwscf.org.

[66] We used the pseudopotentials Si.vbc.UPF from the http://www.quantum-espresso.org distribution.

[67] E. Hult, H. Rydberg, B.I. Lundqvist, and D.C. Langreth, Phys. Rev. B **59**, 4708 (1999).

[68] Q. Wu and W. Yang, J. Chem. Phys. **116**, 515 (2001).

[69] S. L. Richardson, M. Y. Chou, and M. L. Cohen, Phys. Rev. A **31**, 3444 (1985).

[70] F. Gygi and A. Baldereschi Phys. Rev. B **34**, 4405 (1986).

[71] Stefano de Gironcoli (private communication).